Sources of the confusion noise

A. A. Ermash, S. V. Pilipenko, E. V. Mikheeva, V. N. Lukash

Submillimeter and Millimeter Astronomy:
Objectives and Instruments

AstroSpaceCenter, Moscow
12–16 April 2021

The Millimetron Space Telescope

- The Millimetron space telescope will have a 10-m diameter primary mirror
- The main mirror will be actively cooled to the temperature 4.5 K.
- The spacecraft will be launched to the orbit near L2 point of the Earth-Sun system.
- Photometric observations will be carried out with LACS (Long wave Array Camera Spectrometer) and SACS (Short wave Array Camera Spectrometer) instruments.
- SACS will have four bands with following wavelengths: $70\mu m$, $110\mu m$, $250\mu m$, $350\mu m$.
- LACS will have four bands with following wavelengths: $650\mu m$, $850\mu m$, $1100\mu m$, $2000\mu m$.

The model of the CIB

- Recently we have created a model of the infrared background based on the eGALICS simulation (Cousin et al. 2015(a) and Cousin et al. 2015(b)).
- We created a SED library using the GRASIL code by Silva et al. 1998.
- In order to eliminate the effect of "perspective" we used the approach proposed by Blaizot et al. 2005: during the process of the creation of the cone each cube is affected by the following transformations independently on each axis: shift with random distance, rotation to $\pi/2$, π or $-\pi/2$, and reflection along selected axis.
- The detailed description of the model is given in Ermash et al. 2020.

Cubes

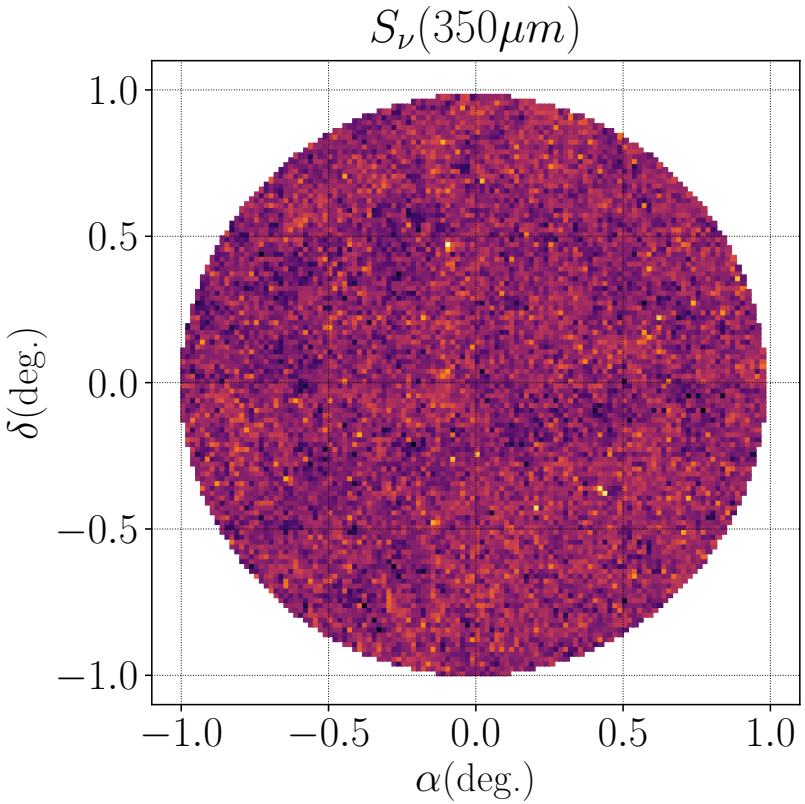
$S_\nu(350\mu m)$
1.0
0.5
0.0
−0.5
−1.0
δ(deg.)
−1.0
−0.5
0.0
0.5
1.0
α(deg.)

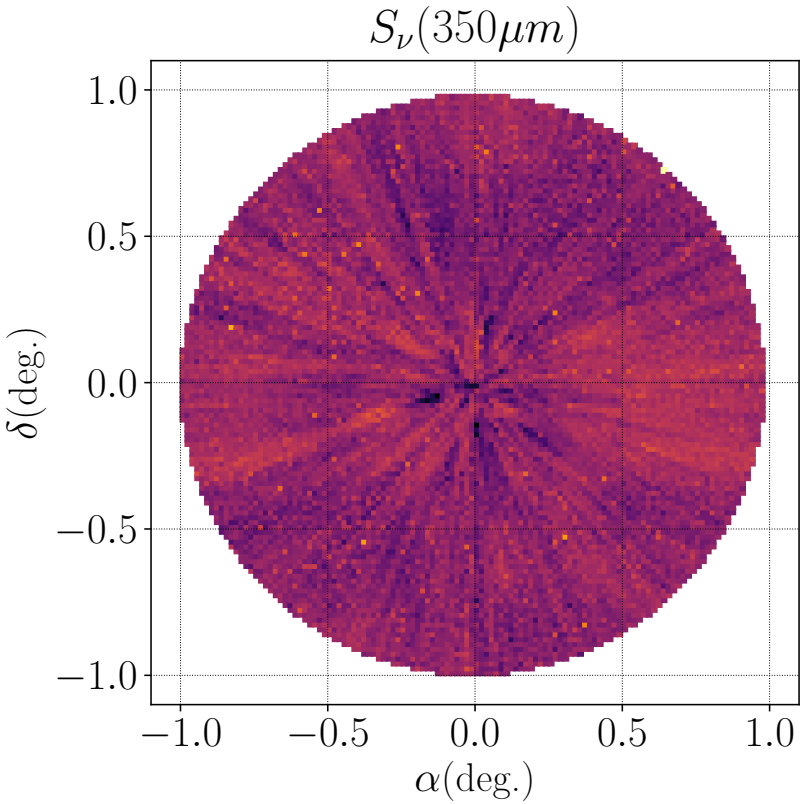
$S_\nu(350\mu m)$
1.0
0.5
0.0
−0.5
−1.0
δ(deg.)
−1.0
−0.5
0.0
0.5
1.0
α(deg.)

Number counts – $70\mu m$.

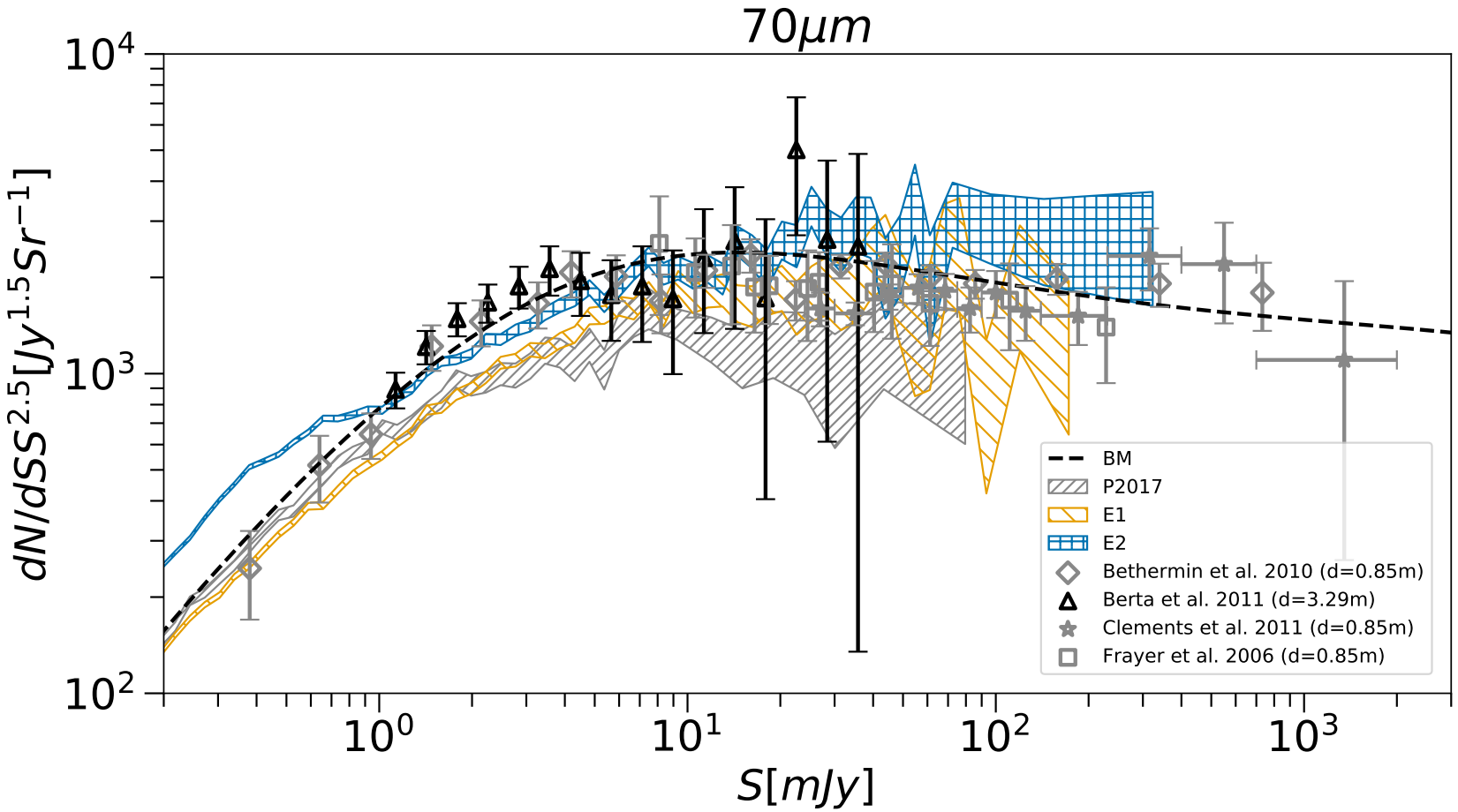

Number counts – $110\mu m$.

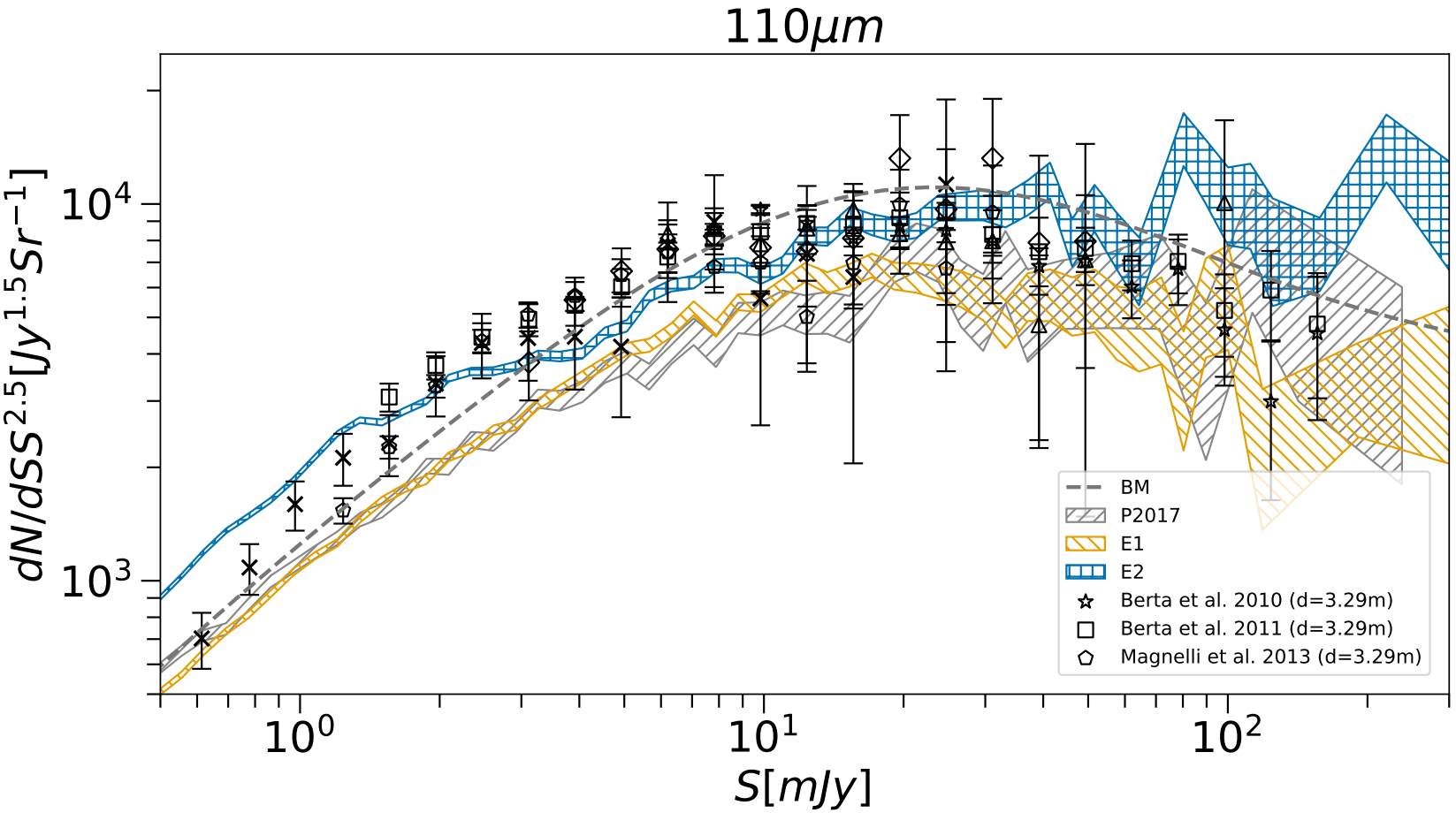

Number counts – 250μm.

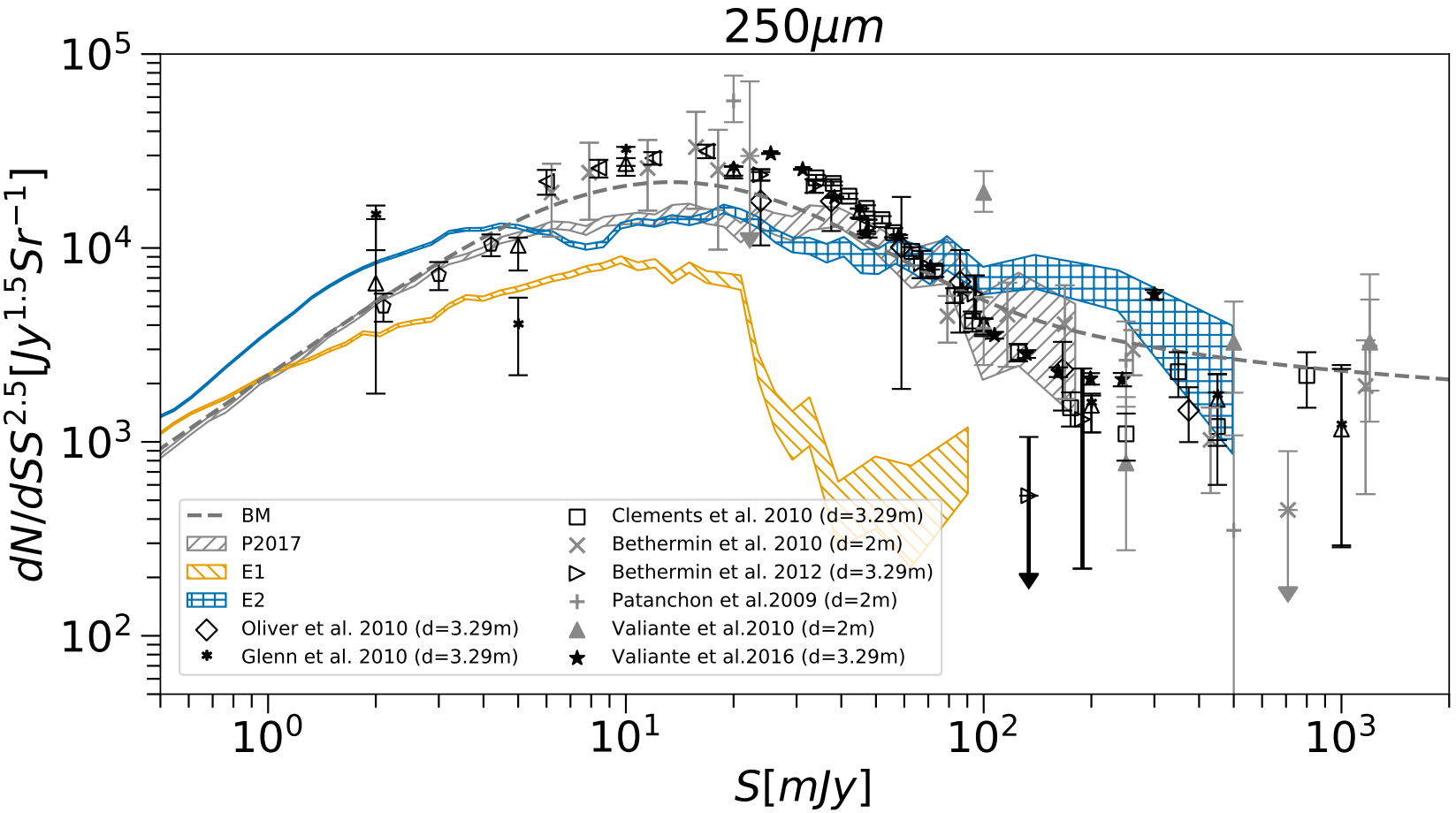

Number counts – 350μm.

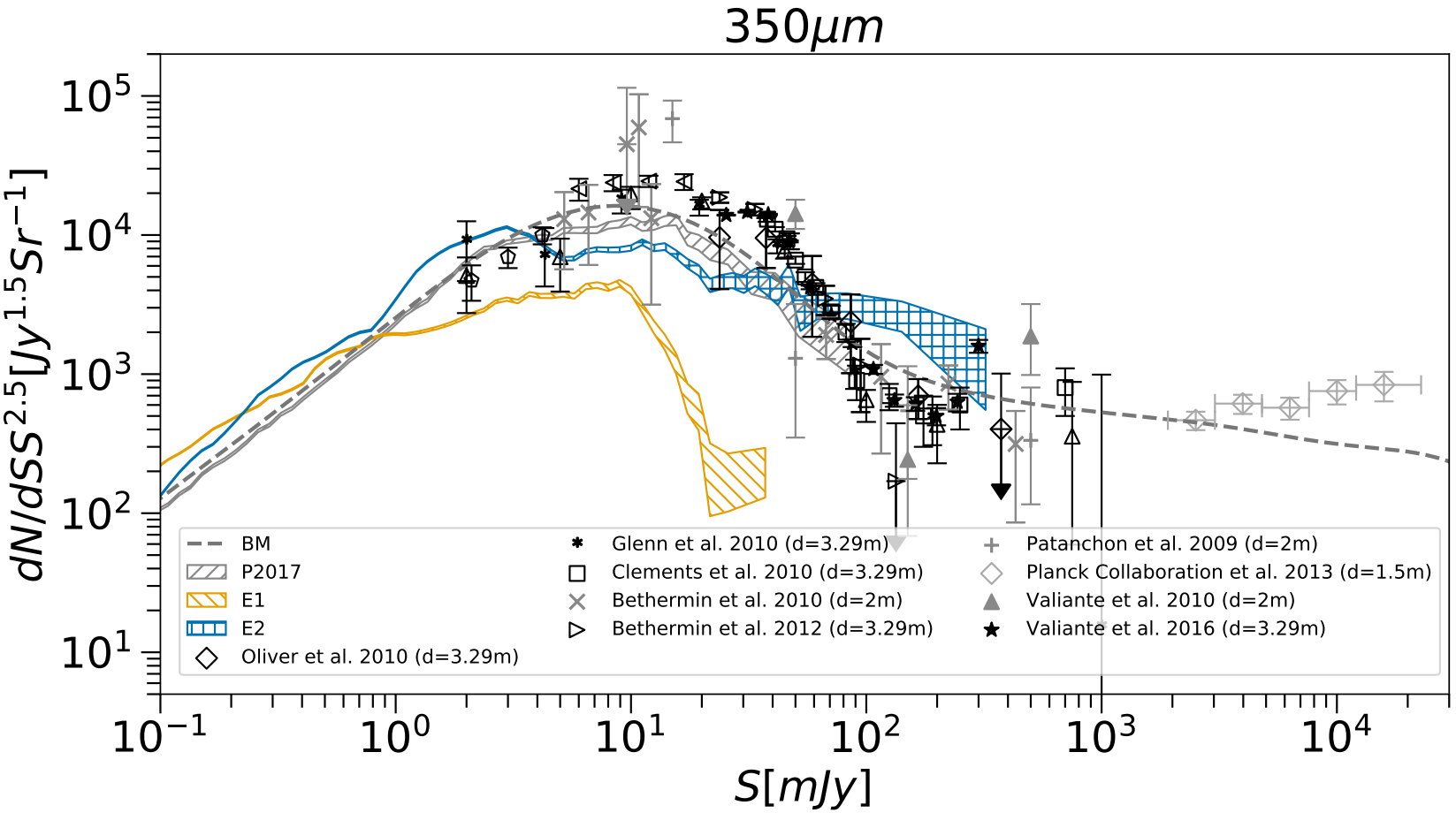

Number counts – 650μm.

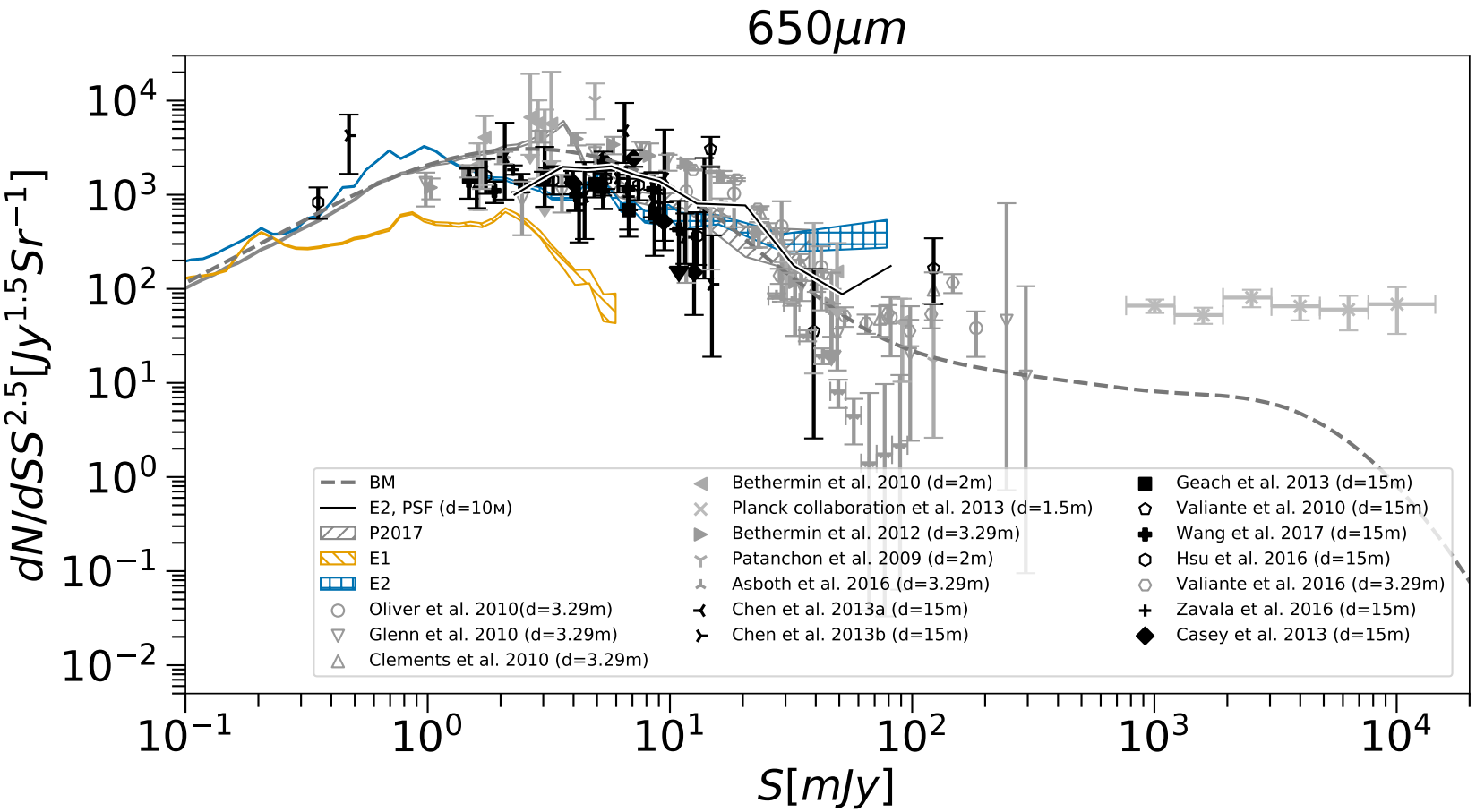

Number counts – 850μm.

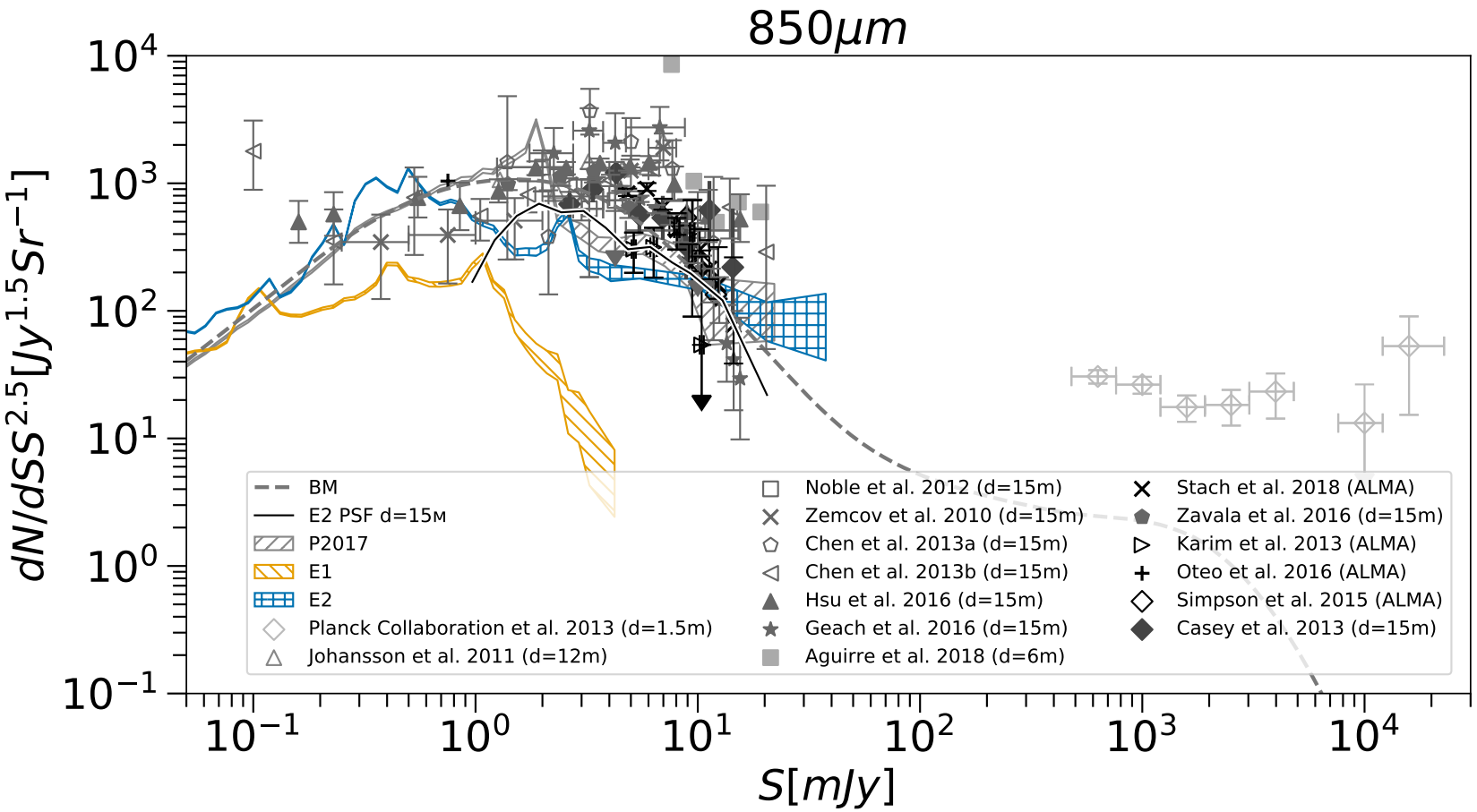

Number counts – 1100μm.

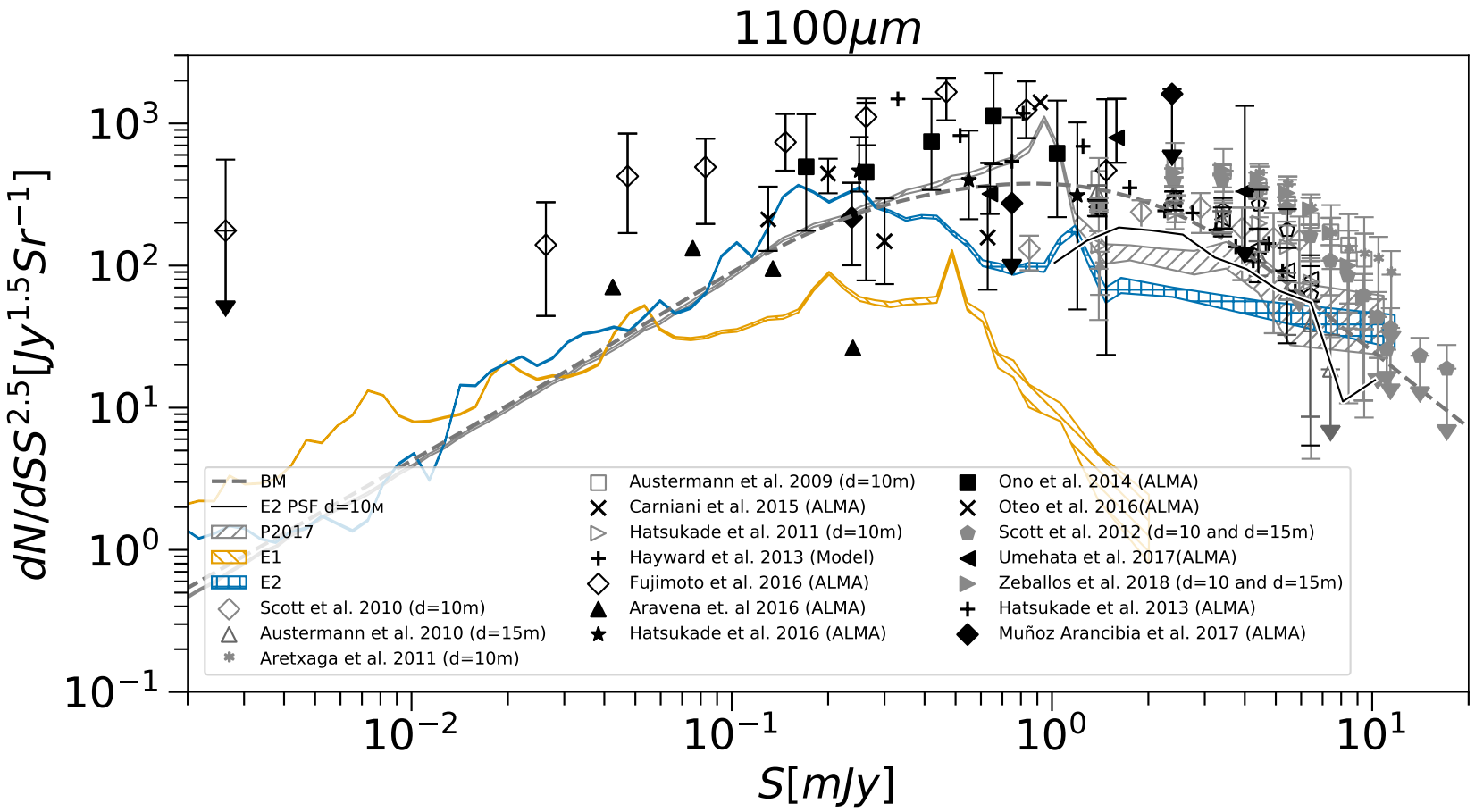

Number counts – $2000\mu m$.

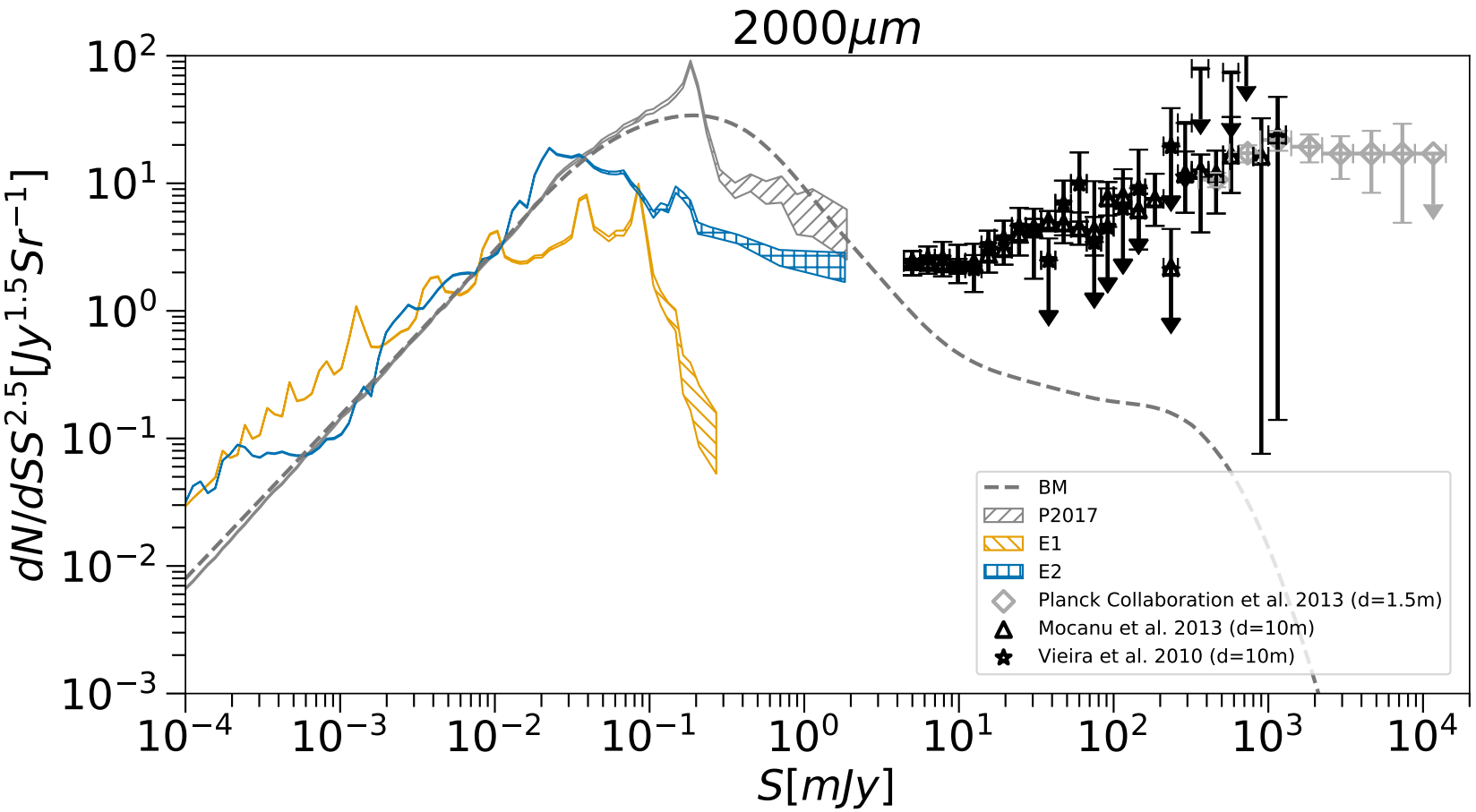

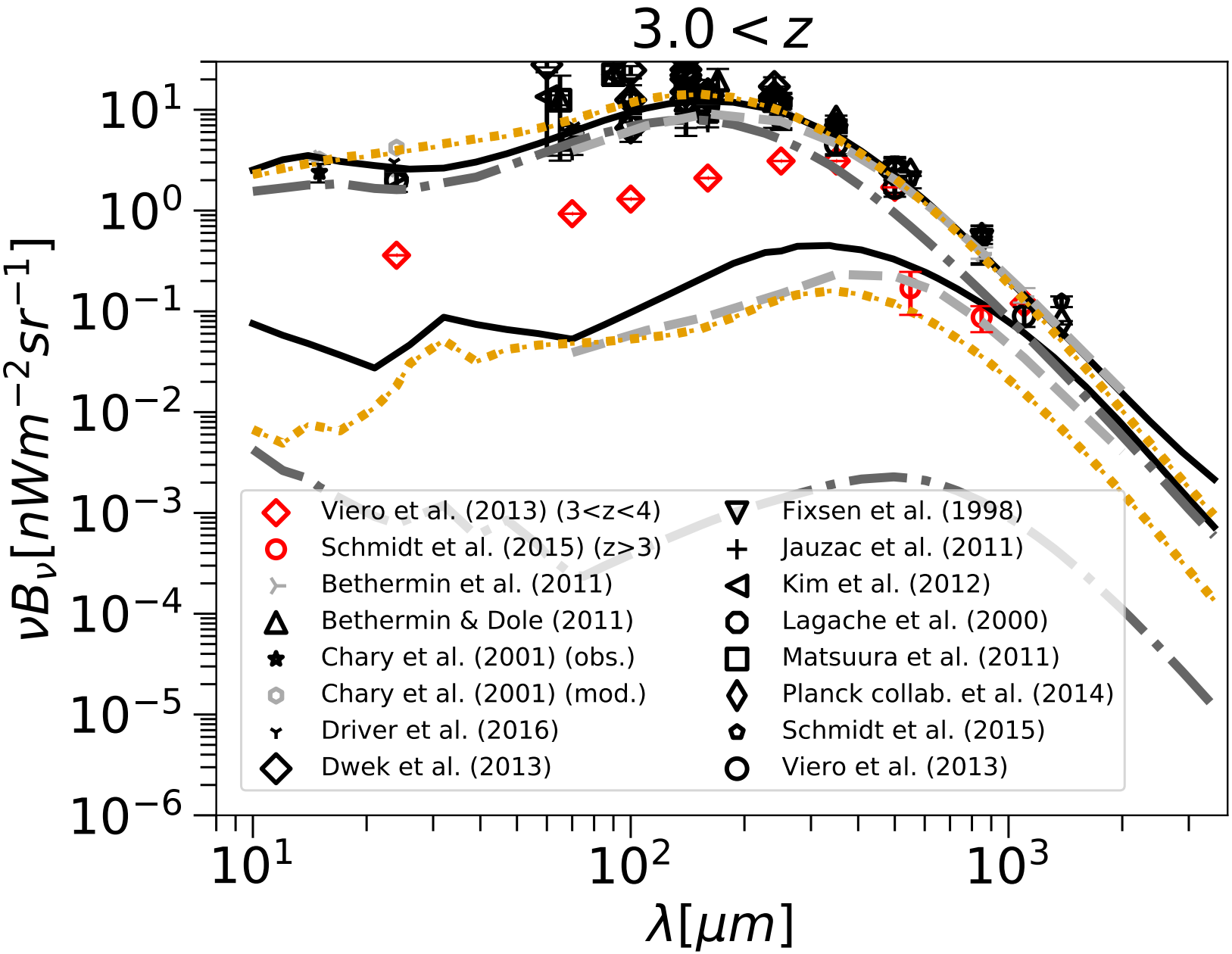
3.0 < z
$\nu B_\nu [nWm^{-2}sr^{-1}]$
$\lambda [\mu m]$
10^{1}
10^{0}
10^{-1}
10^{-2}
10^{-3}
10^{-4}
10^{-5}
10^{-6}
10^{1}
10^{2}
10^{3}
Viero et al. (2013) (3<z<4)
Schmidt et al. (2015) (z>3)
Bethermin et al. (2011)
Bethermin & Dole (2011)
Chary et al. (2001) (obs.)
Chary et al. (2001) (mod.)
Driver et al. (2016)
Dwek et al. (2013)
Fixsen et al. (1998)
Jauzac et al. (2011)
Kim et al. (2012)
Lagache et al. (2000)
Matsuura et al. (2011)
Planck collab. et al. (2014)
Schmidt et al. (2015)
Viero et al. (2013)

The problem of confusion

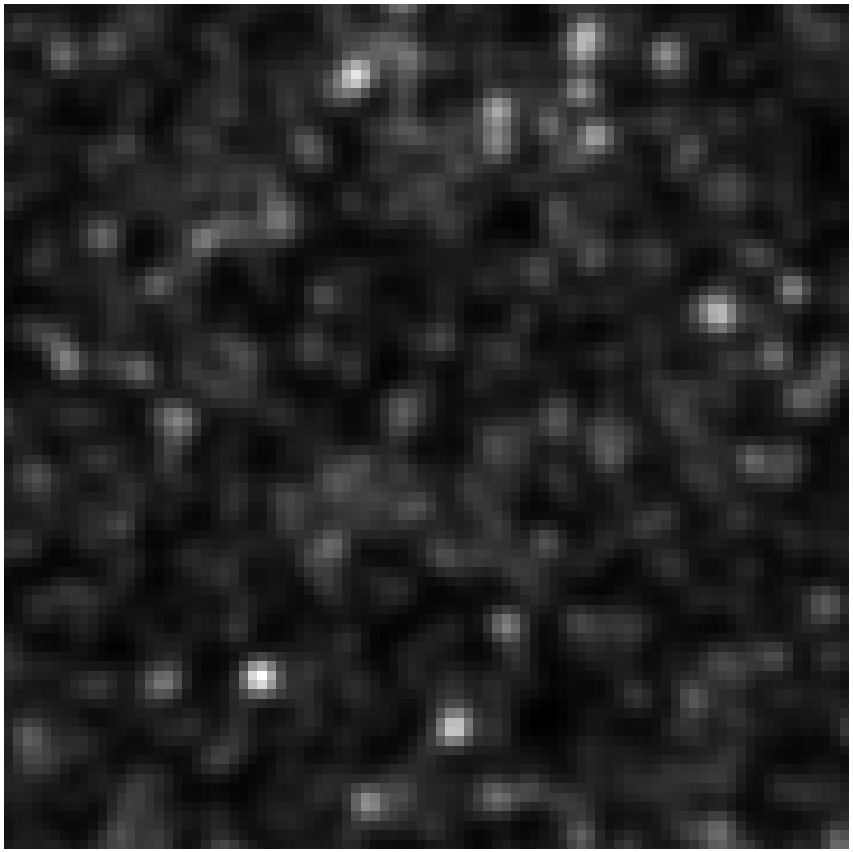

Model map for the $850\mu m$ waveband. Diameter of the main mirror $d = 10m$ (Millimetron). Angular size 10×10 angular minutes.

Estimates of the confusion noise

There are several ways to define the confusion noise. They can be divided into two categories

1. Based on the information about the number counts.
2. Based on the analysis of the model maps.

The easiest way to estimate the confusion noise from the model maps is to simply measure the flux dispersion in pixels. The major drawback of such an approach is that it will significantly overestimate the confusion noise due to the presence of bright resolved objects that contribute to the total flux but not to confusion. The validity of such an approach is questionable because the flux distribution in pixels is non-Gaussian (H. T. Nguyen, B. Schulz et al., 2010; G. Marsden, P. A. R. Ade et al., 2009.; R. Leiton, D. Elbaz et al., 2015.)

Estimates of the confusion noise

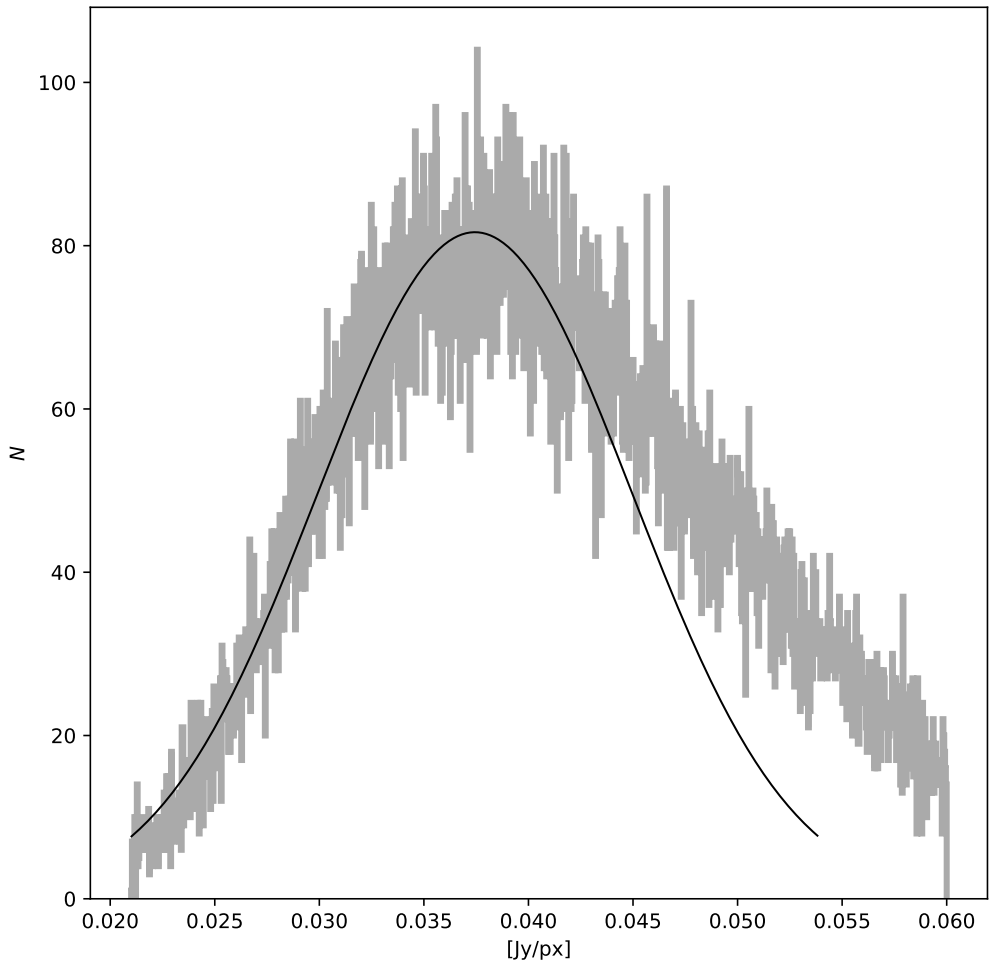

In some papers (see, e.g., Marsden et al. 2009) the confusion noise is defined as σ of the Gaussian fitted to the left side of the pixel

Effects of the creation of the cone

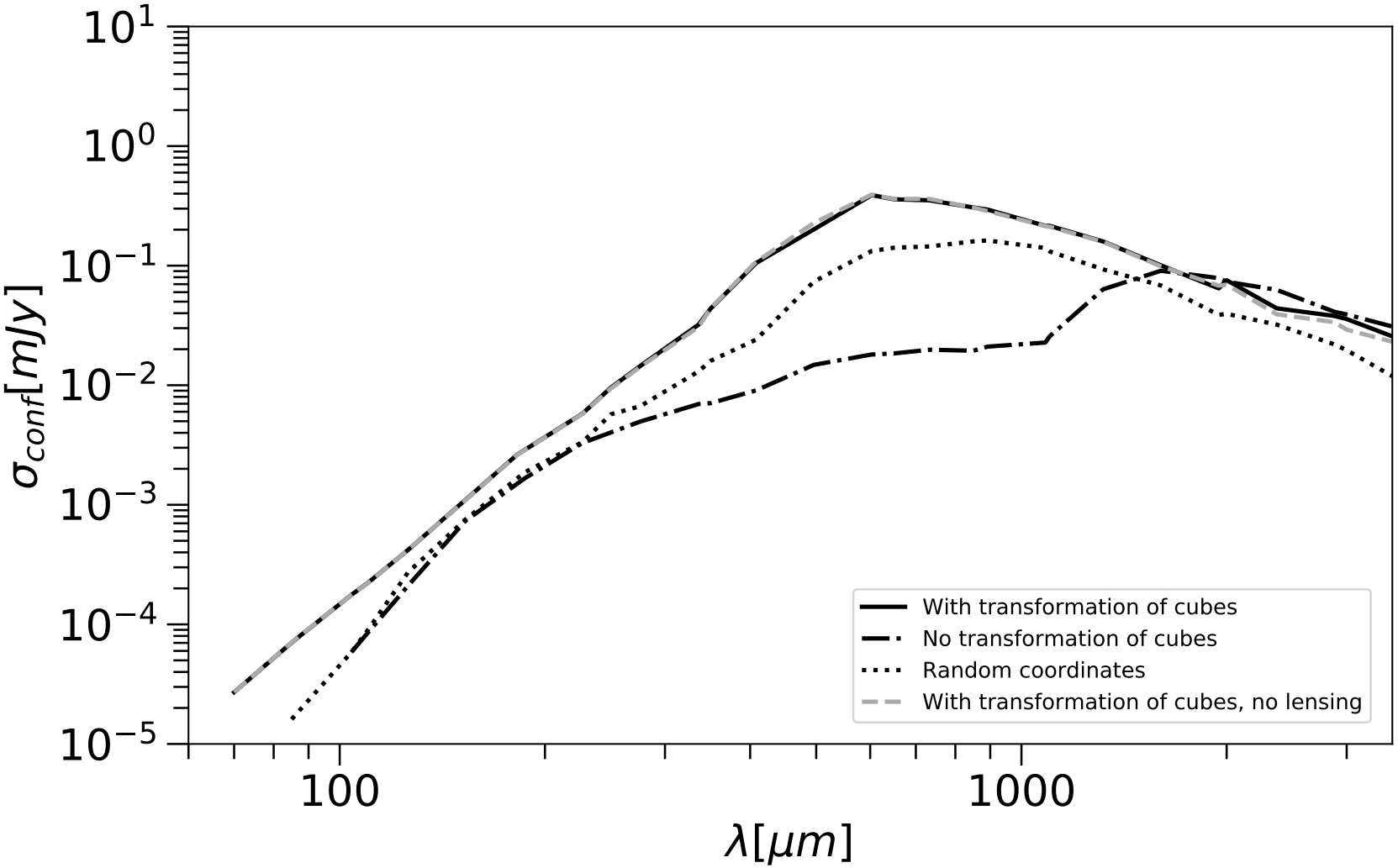

Confusion noise estimations for Millimetron

Wavelength, μm	Confusion noise	
	σ, mJy	$FWHM/2.355$, mJy
70	$2.51 \pm 0.07 \times 10^{-5}$	$2.79 \pm 0.08 \times 10^{-5}$
110	$2.40 \pm 0.07 \times 10^{-4}$	$2.68 \pm 0.08 \times 10^{-4}$
250	$9.69 \pm 0.48 \times 10^{-3}$	$1.07 \pm 0.05 \times 10^{-2}$
350	$4.44 \pm 0.46 \times 10^{-2}$	$4.88 \pm 0.53 \times 10^{-2}$
650	$3.26 \pm 0.17 \times 10^{-1}$	$3.59 \pm 0.20 \times 10^{-1}$
850	$2.99 \pm 0.15 \times 10^{-1}$	$3.21 \pm 0.18 \times 10^{-1}$
1100	$2.19 \pm 0.07 \times 10^{-1}$	$2.34 \pm 0.08 \times 10^{-1}$
2000	$7.95 \pm 0.44 \times 10^{-2}$	$8.19 \pm 0.53 \times 10^{-2}$

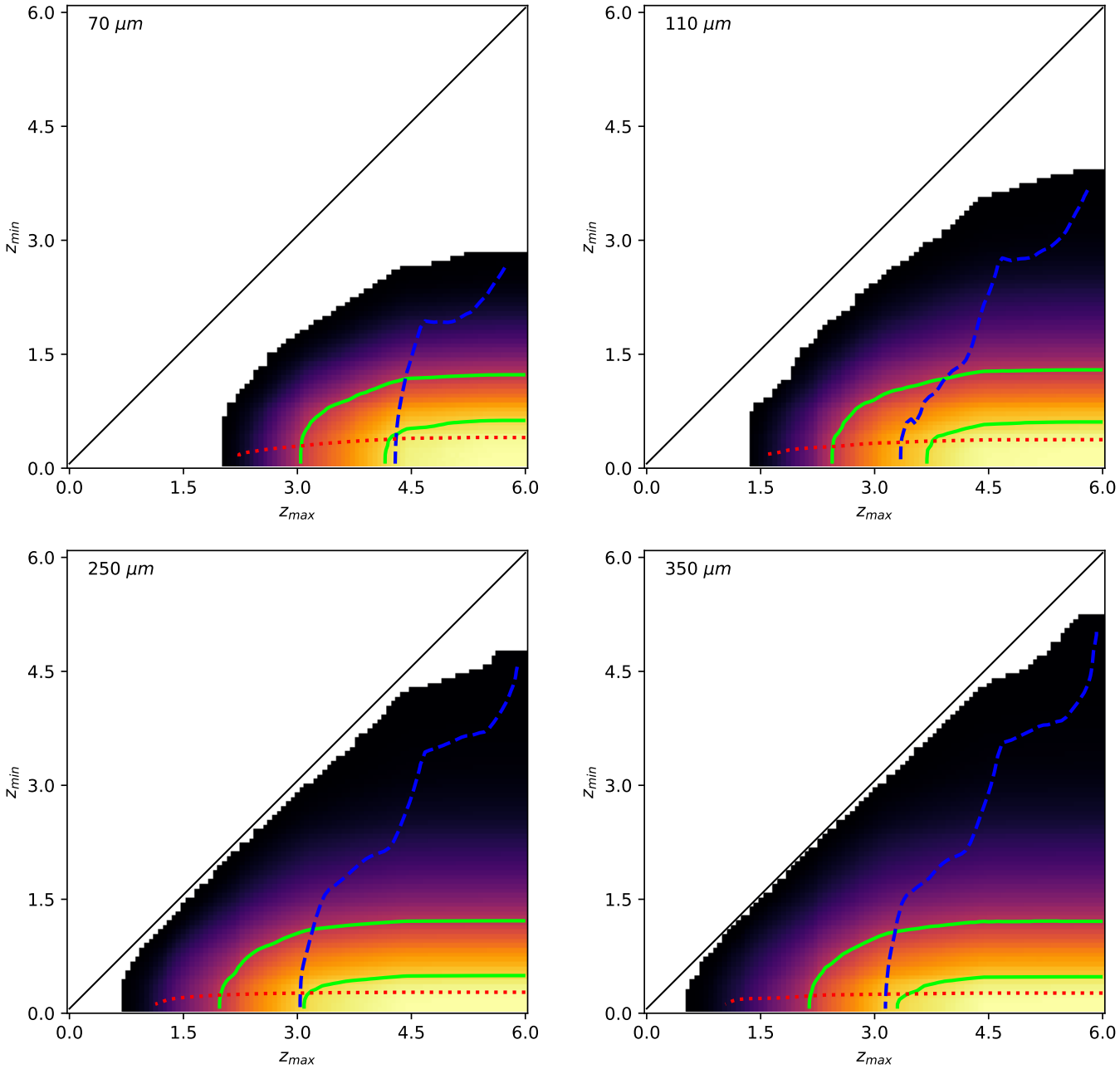
70 μm
110 μm
250 μm
350 μm
z_{min}
z_{max}
0.0
1.5
3.0
4.5
6.0

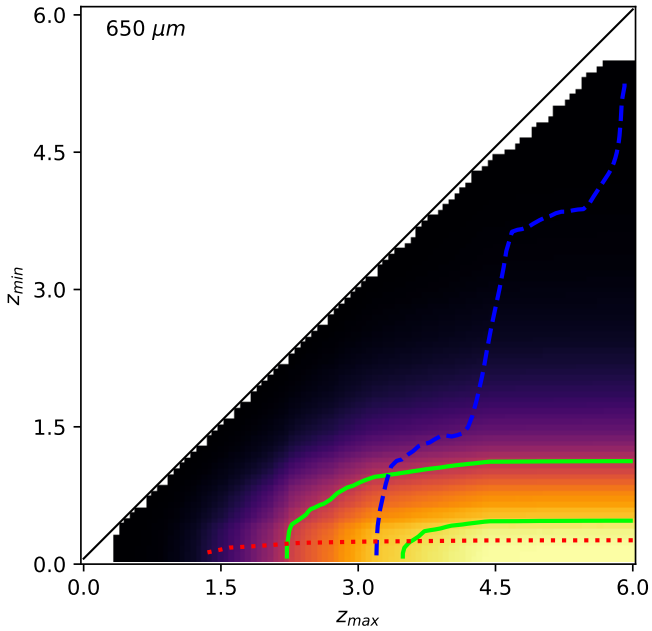
650 μm
z_{min}
z_{max}
0.0
1.5
3.0
4.5
6.0

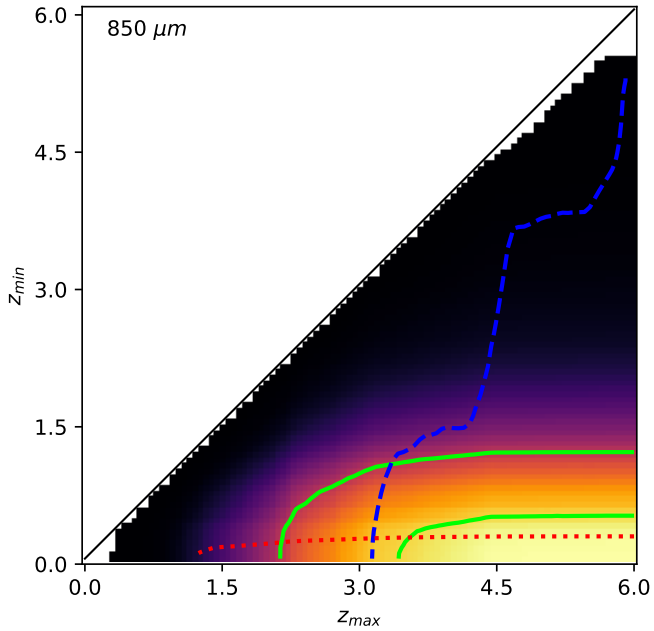
850 μm
z_{min}
z_{max}
0.0
1.5
3.0
4.5
6.0

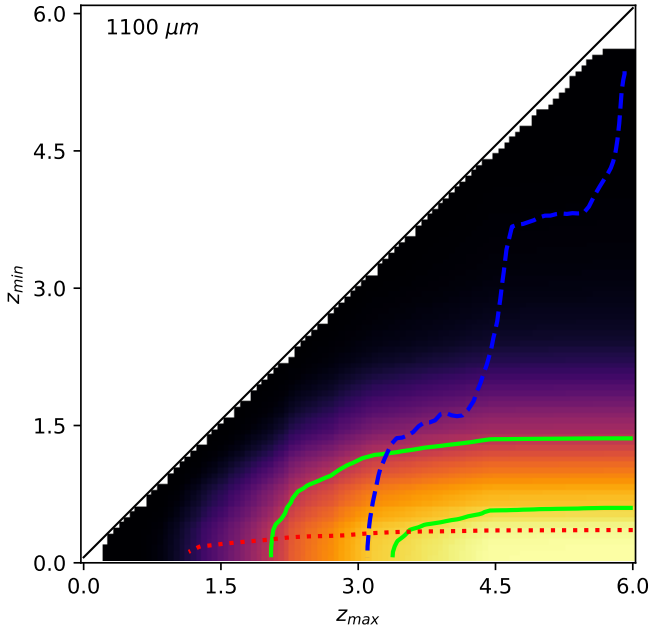
1100 μm
z_{min}
z_{max}
0.0
1.5
3.0
4.5
6.0

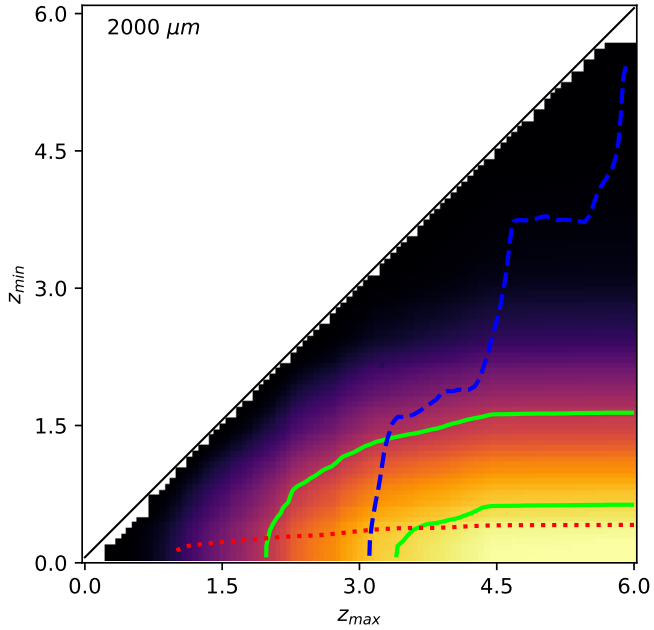
2000 μm
z_{min}
z_{max}
0.0
1.5
3.0
4.5
6.0

λ,	I		II	
μm	z_{min}	z_{max}	z_{min}	z_{max}
70	0.62	4.11	0.36	4.25
110	0.60	3.65	0.36	3.32
250	0.49	3.06	0.24	3.01
350	0.47	3.27	0.24	3.12
650	0.47	3.45	0.24	3.17
850	0.52	3.39	0.30	3.12
1100	0.59	3.34	0.30	3.08
2000	0.63	3.37	0.36	3.10

Redshift intervals that contribute the most to the confusion noise.

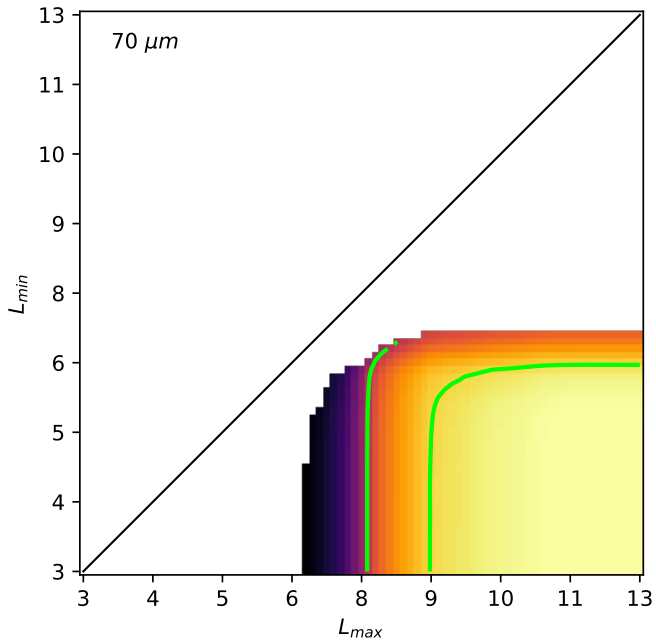
70 μm
L_{min}
L_{max}

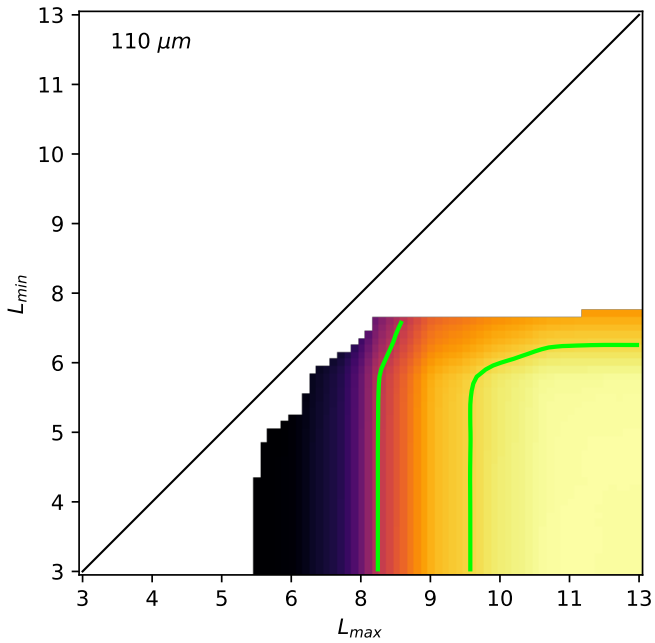
110 μm
L_{min}
L_{max}

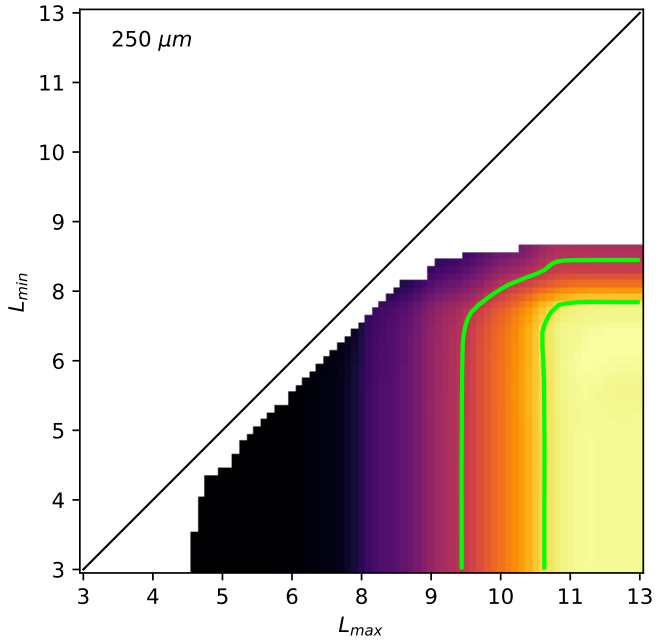
250 μm
L_{min}
L_{max}

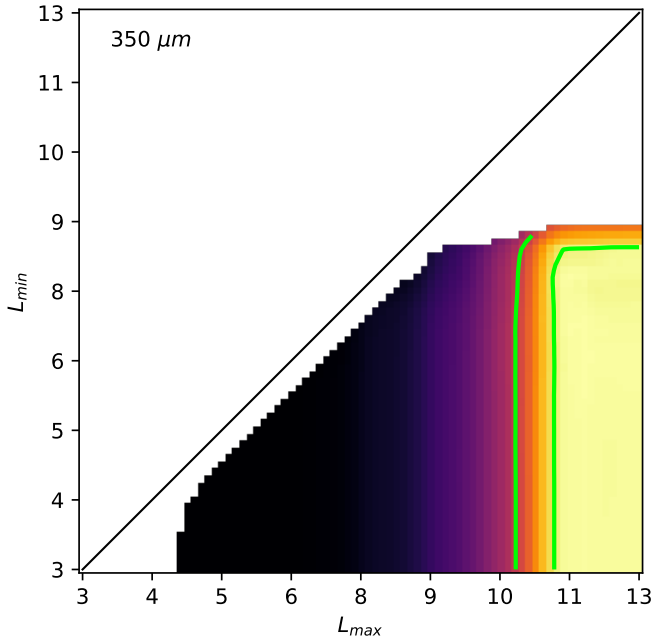
350 μm
L_{min}
L_{max}

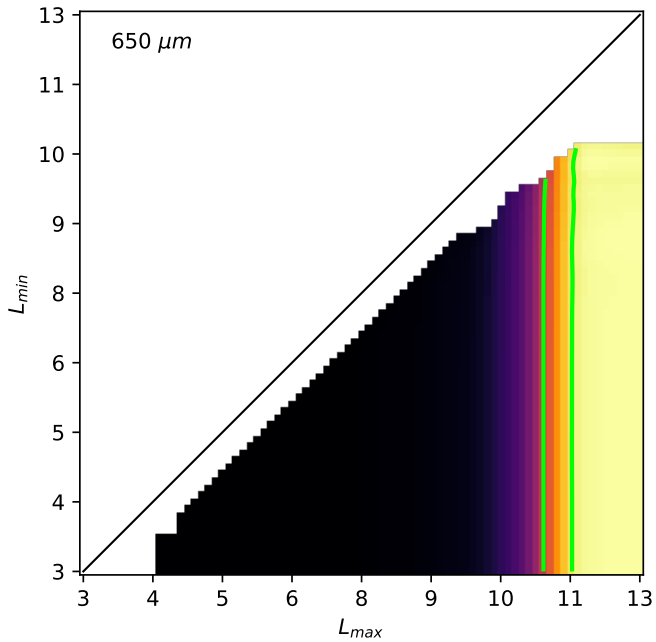
650 μm
L_{min}
L_{max}

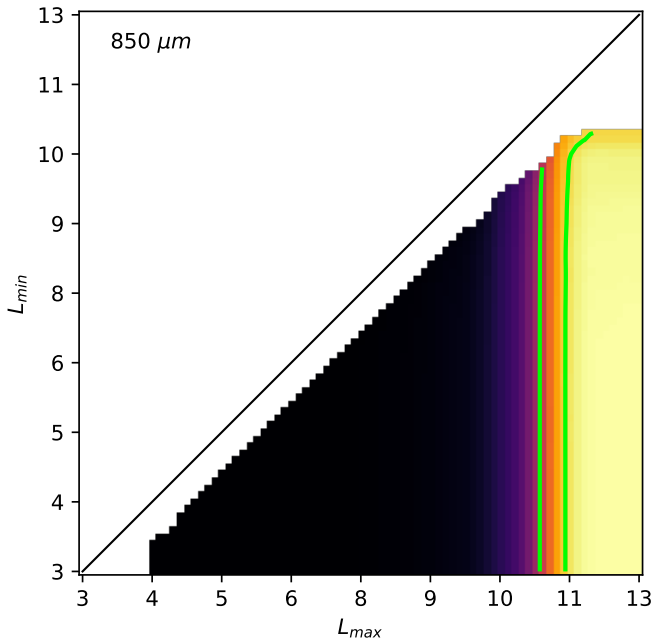
850 μm
L_{min}
L_{max}

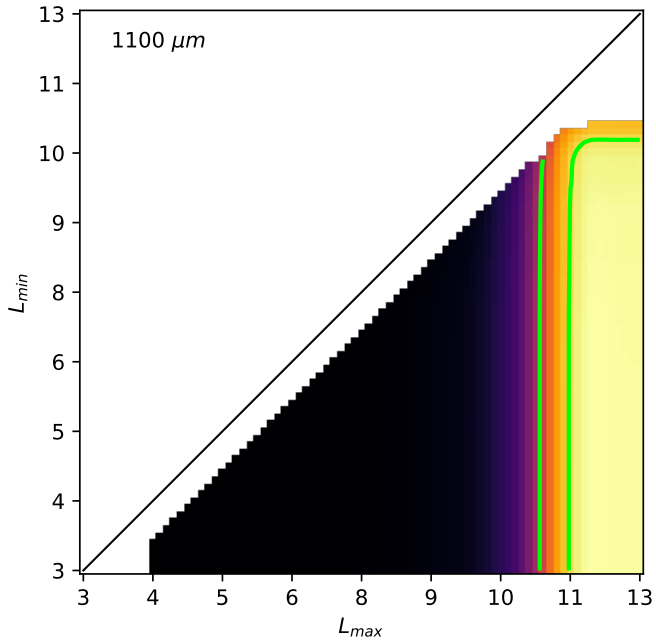
1100 μm
L_{min}
L_{max}

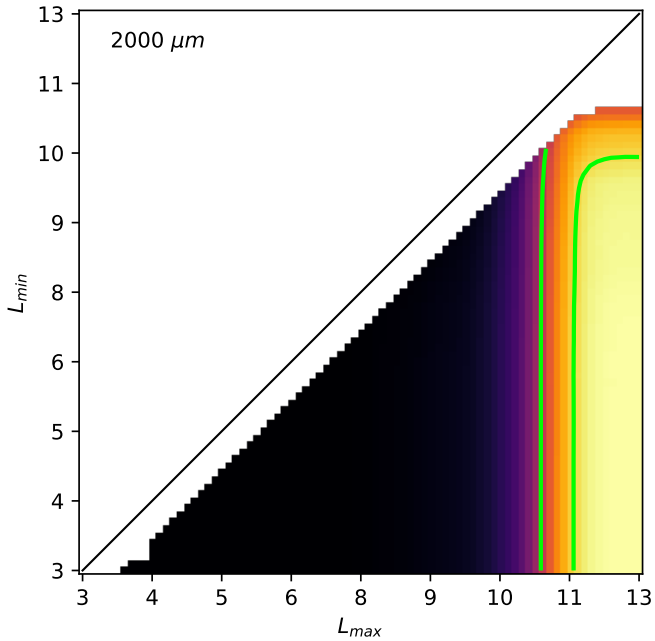
2000 μm
L_{min}
L_{max}

λ, μm	$\log_{10}(L_{min}/L_{\odot})$	$\log_{10}(L_{max}/L_{\odot})$
70	6.88	9.10
110	7.08	9.90
250	8.06	11.15
350	9.31	12.01
650	10.74	11.58
850	11.12	11.56
1100	11.24	12.24
2000	10.38	11.69

Luminosity range of galaxies than contribute 90% to the confusion noise.

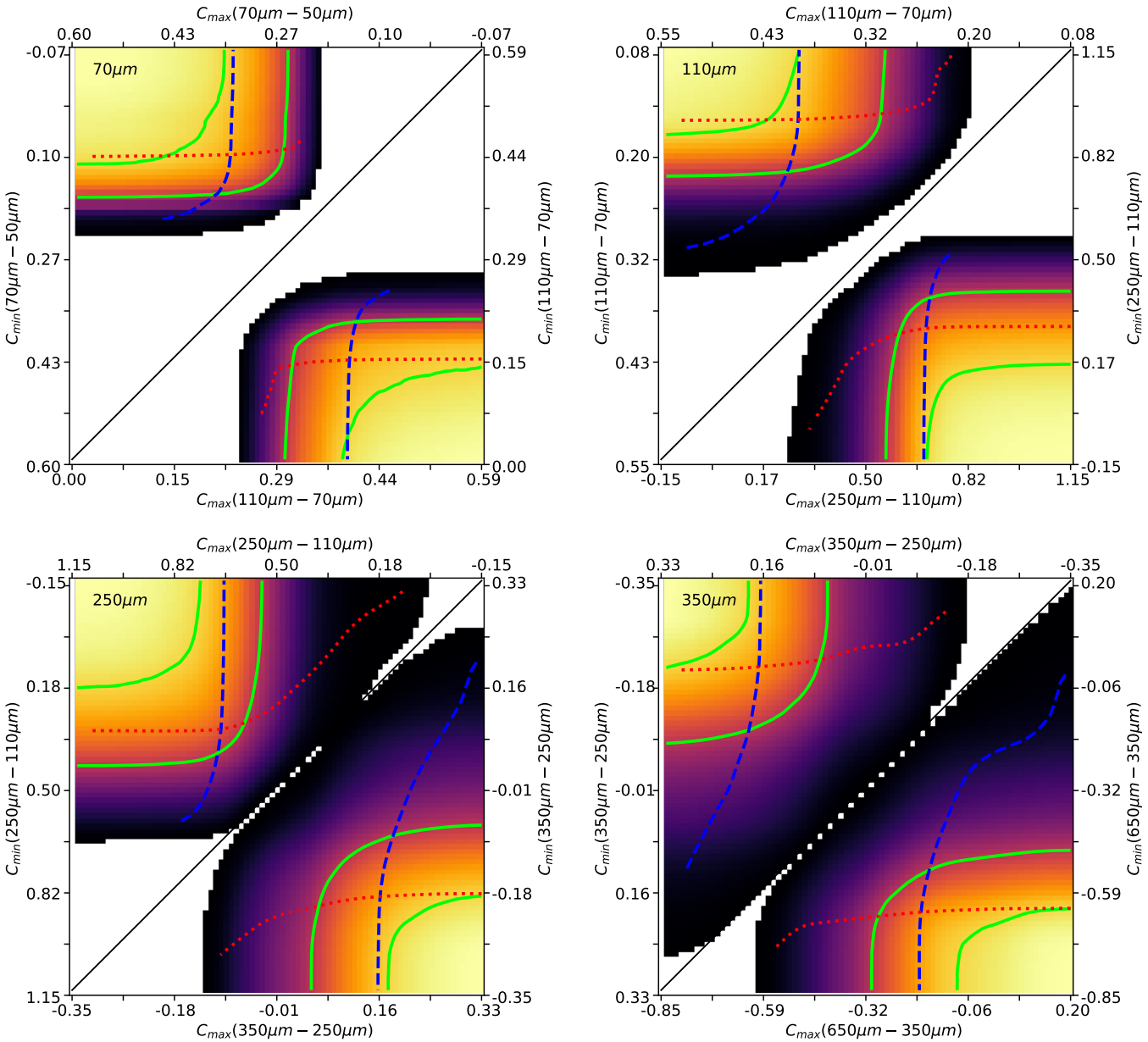
$C_{max}(70\mu m - 50\mu m)$
$C_{min}(70\mu m - 50\mu m)$
$C_{max}(110\mu m - 70\mu m)$
$C_{min}(110\mu m - 70\mu m)$
70μm
$C_{max}(110\mu m - 70\mu m)$
$C_{min}(110\mu m - 70\mu m)$
$C_{max}(250\mu m - 110\mu m)$
$C_{min}(250\mu m - 110\mu m)$
110μm
$C_{max}(250\mu m - 110\mu m)$
$C_{min}(250\mu m - 110\mu m)$
$C_{max}(350\mu m - 250\mu m)$
$C_{min}(350\mu m - 250\mu m)$
250μm
$C_{max}(350\mu m - 250\mu m)$
$C_{min}(350\mu m - 250\mu m)$
$C_{max}(650\mu m - 350\mu m)$
$C_{min}(650\mu m - 350\mu m)$
350μm

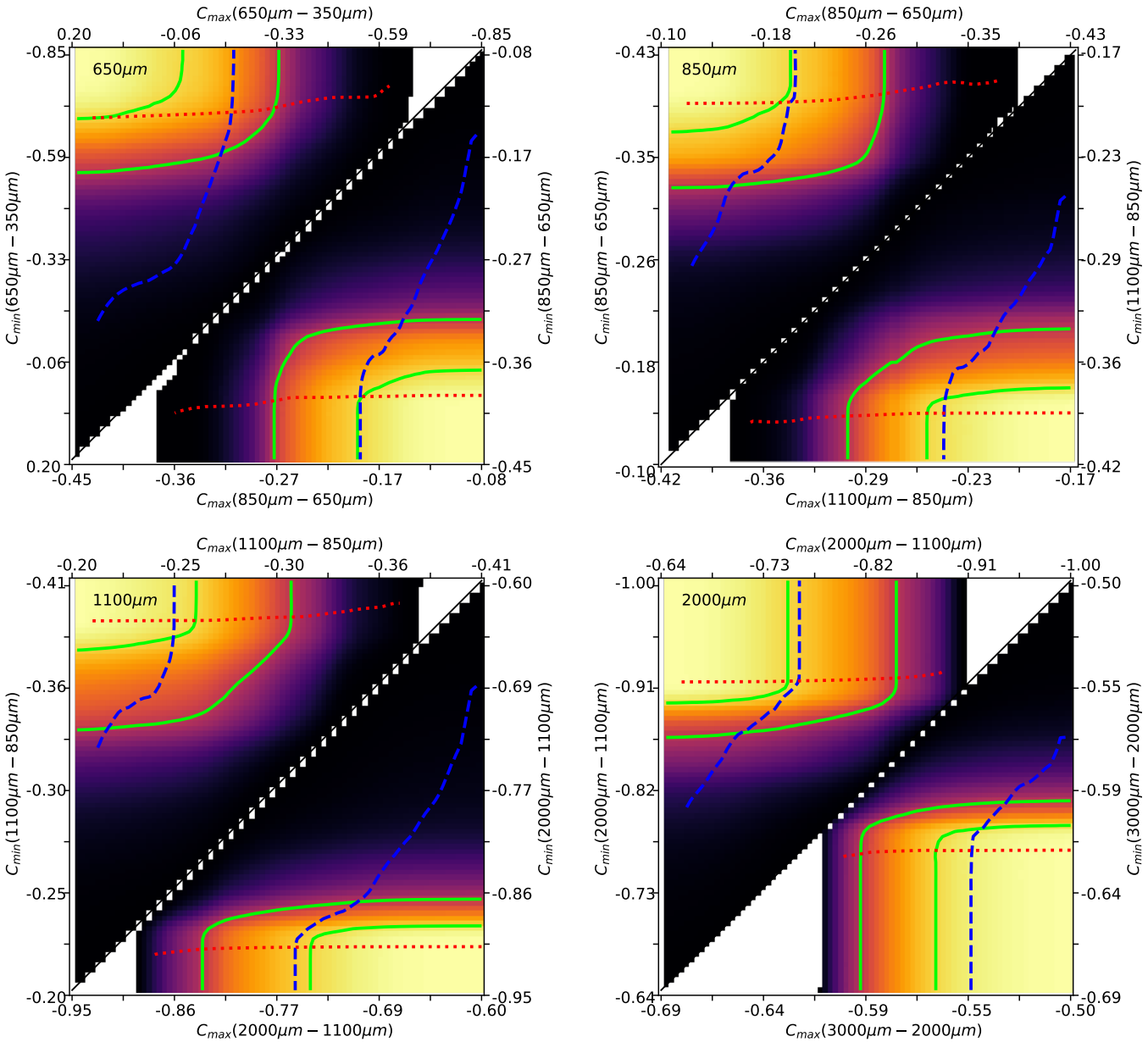
$C_{max}(650\mu m - 350\mu m)$
$C_{min}(650\mu m - 350\mu m)$
$C_{min}(850\mu m - 650\mu m)$
$C_{max}(850\mu m - 650\mu m)$
650μm
$C_{max}(850\mu m - 650\mu m)$
$C_{min}(850\mu m - 650\mu m)$
$C_{min}(1100\mu m - 850\mu m)$
$C_{max}(1100\mu m - 850\mu m)$
850μm
$C_{max}(1100\mu m - 850\mu m)$
$C_{min}(1100\mu m - 850\mu m)$
$C_{min}(2000\mu m - 1100\mu m)$
$C_{max}(2000\mu m - 1100\mu m)$
1100μm
$C_{max}(2000\mu m - 1100\mu m)$
$C_{min}(2000\mu m - 1100\mu m)$
$C_{min}(3000\mu m - 2000\mu m)$
$C_{max}(3000\mu m - 2000\mu m)$
2000μm

Values C_{min} and C_{max} in columns 4 and 5 limit 90% contribution to the confusion noise. Columns 6 and 7 define area where the derivative of the confusion noise is lower than certain threshold.

λ_r, μm	λ_0, μm	λ_1, μm	I		II	
			C_{min}	C_{max}	C_{min}	C_{max}
70	70	110	0.14	0.38	0.15	0.39
70	50	70	0.11	0.35	0.10	0.34
110	110	250	0.16	0.68	0.28	0.68
110	70	110	0.18	0.39	0.16	0.39
250	250	350	-0.19	0.17	-0.19	0.16
250	110	250	0.19	0.75	0.32	0.68
350	350	650	-0.63	-0.10	-0.64	-0.19
350	250	350	-0.21	0.19	-0.21	0.17
650	650	850	-0.37	-0.20	-0.39	-0.19
650	350	650	-0.68	-0.08	-0.69	-0.20
1100	1100	2000	-0.89	-0.75	-0.91	-0.76
1100	850	1100	-0.37	-0.26	-0.39	-0.25
2000	2000	3000	-0.61	-0.56	-0.62	-0.55
2000	1100	2000	-0.89	-0.75	-0.91	-0.76

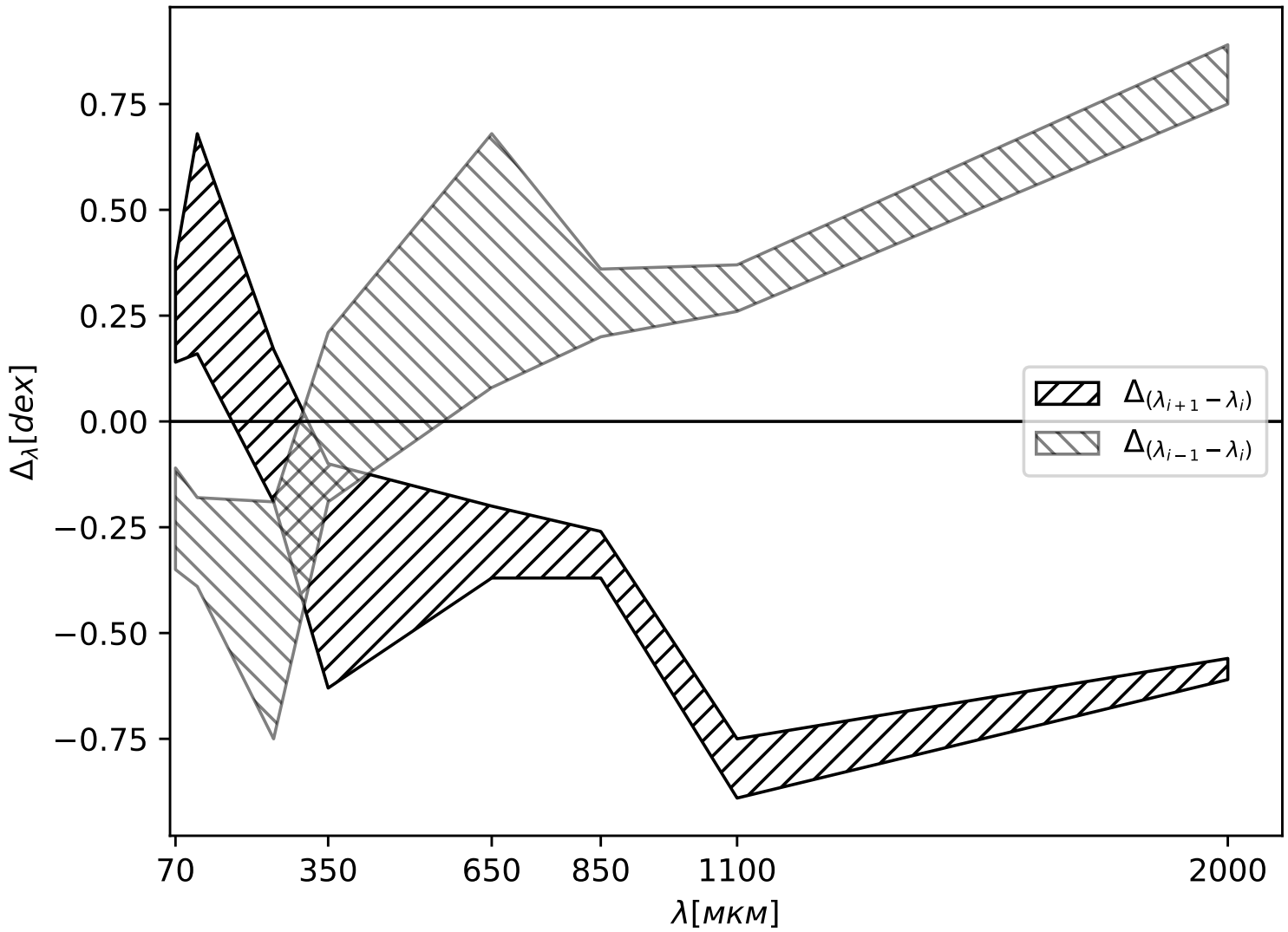

Color interval of objects contributing 90% to the confusion noise vs wavelength.

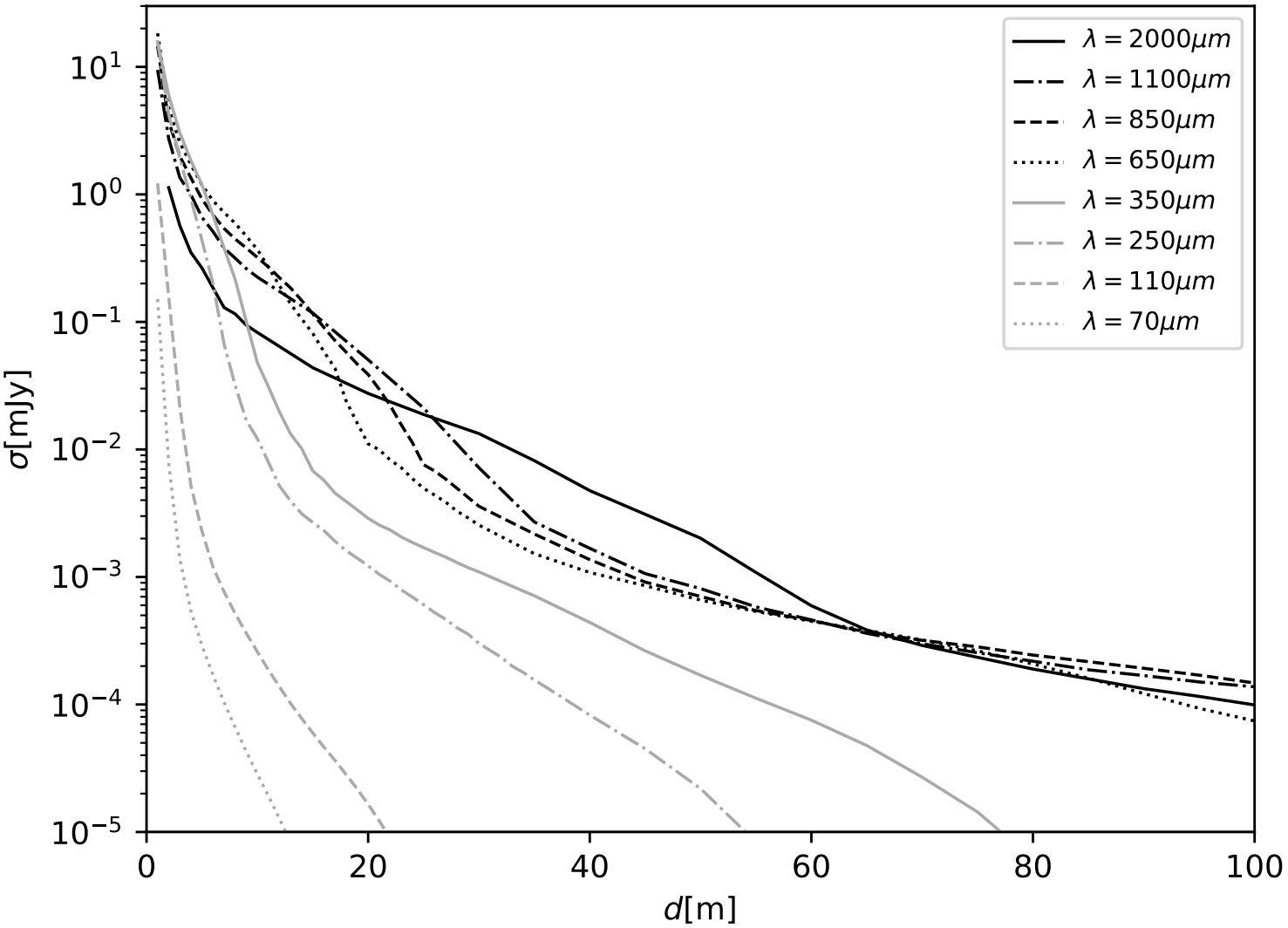

Confusion noise vs diameter of the main mirror.

Conclusions

1. Large scale structure is crucial in creating a model of the confusion noise.
2. Gravitational lensing plays minor role in confusion noise
3. The following answer can be given to the question "At what redshifts objects contribute the most to the confusion noise": lower redshift boundary does not depend on wavelength $z_{min} \sim 0.5 - 0.6$ while upper boundary gradually decreases from ~ 4 to ~ 3 if we move from $70\mu m$ to $2000\mu m$.
4. At short wavelengths $10^7 L_\odot$ – $10^9 L_\odot$ objects give the most contribution, while at large wavelengths confusion is created mostly by $L \geq 10^{10} L_\odot$.
5. At short wavelengths the confusion noise is created by objects that give large contribution to confusion in closest longer waveband and relatively small contribution into confusion in closest shorter waveband. And larger wavelengths the situation gradually changes to the opposite.

Bibliography - 1

- M. Cousin, G. Lagache et al. Galaxy stellar mass assembly: the difficulty matching observations and semi-analytical predictions. Astronomy and Astrophysics, 575:A32, March 2015.
- M. Cousin, G. Lagache et al. Towards a new modelling of gas flows in a semi-analytical model
- L. Silva, G. L. Granato et al. Modeling the Effects of Dust on Galactic Spectral Energy Distributions from the Ultraviolet to the Millimeter Band. Astrophys. J, 509:103–117, December 1998.
- J. Blaizot, Y. Wadadekar et al. MoMaF: the Mock Map Facility. MNRAS, 360:159–175, June 2005.
- A. A. Ermash, S. V. Pilipenko and V. N. Lukash. Astronomy Letters 46 , 298 (2020) (arXiv:1812.08575)
- H. T. Nguyen, B. Schulz et al. HerMES: The SPIRE confusion limit. Astronomy and Astrophysics, 518:L5, July 2010.
- G. Marsden, P. A. R. Ade et al. BLAST: Resolving the Cosmic Submillimeter Background. Astrophys. J, 707:1729-1739, December 2009.

Bibliography - 2

- R. Leiton, D. Elbaz et al.. GOODS-Herschel: identification of the individual galaxies responsible for the 80-290 μm cosmic infrared background. Astronomy and Astrophysics, 579:A93, July 2015.

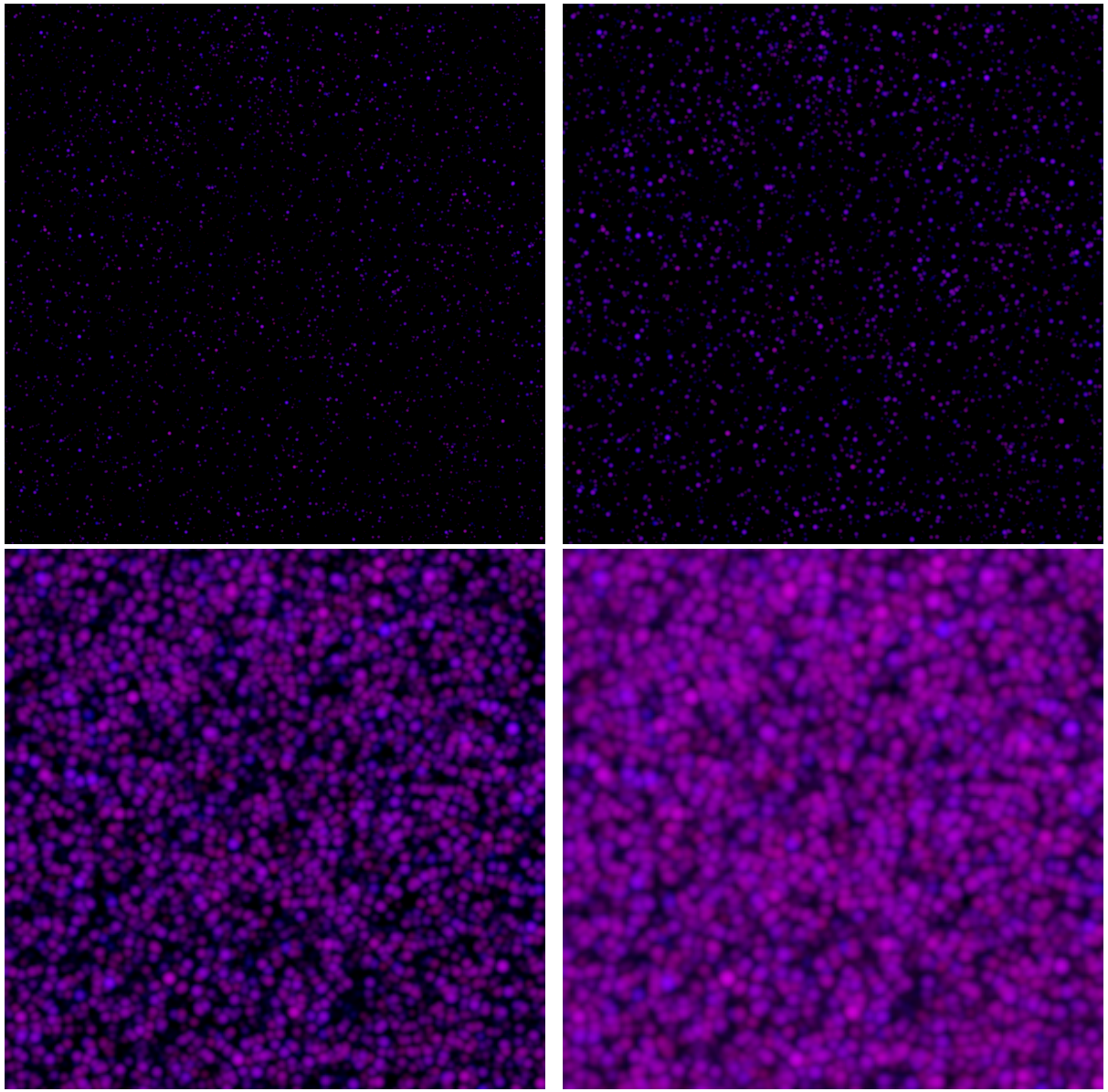

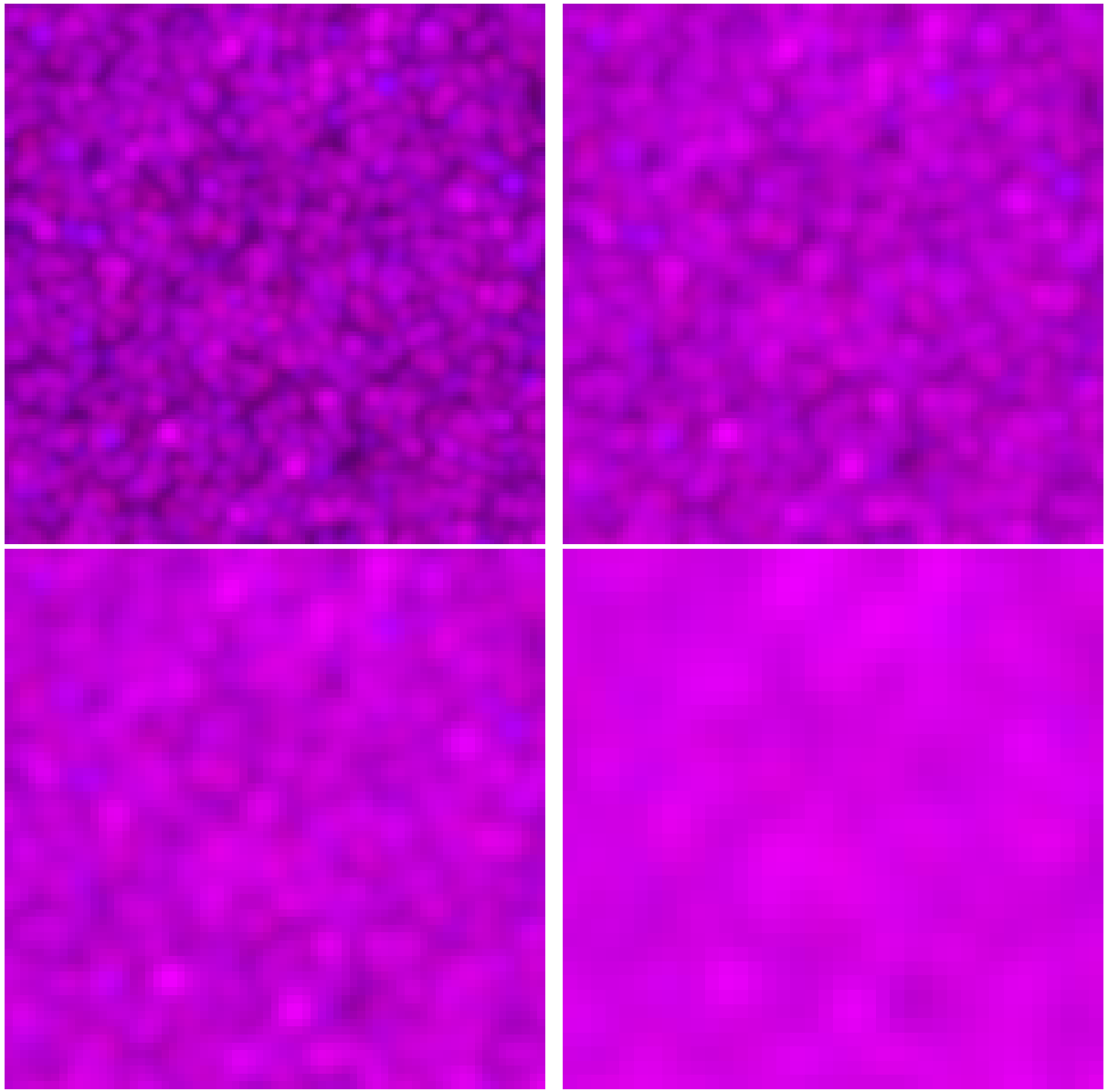

R – 350μm, G – 110μm, B – 70μm

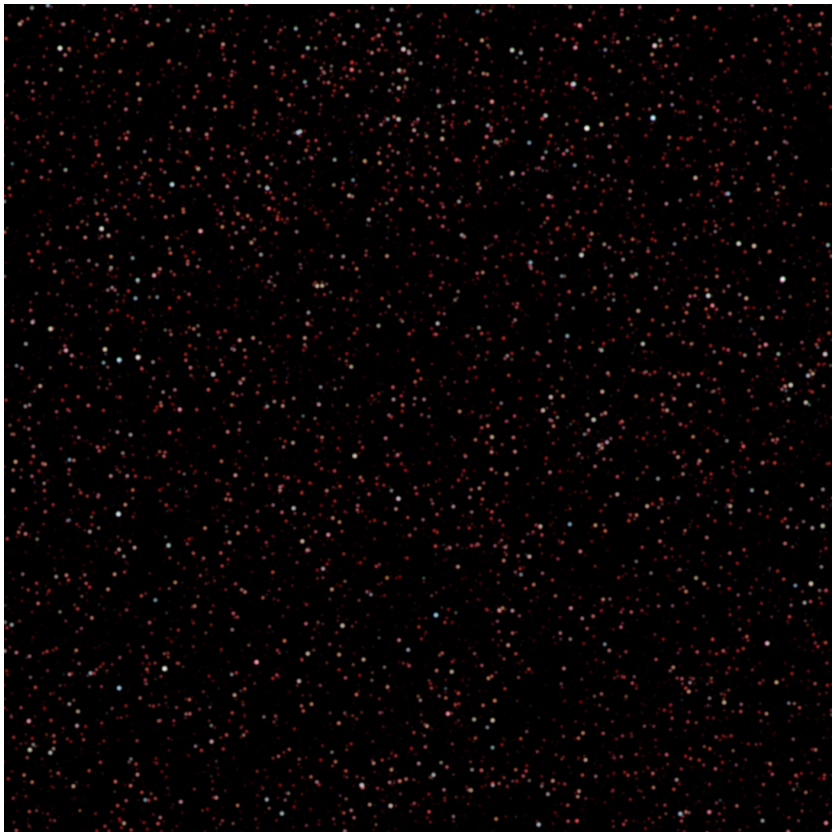

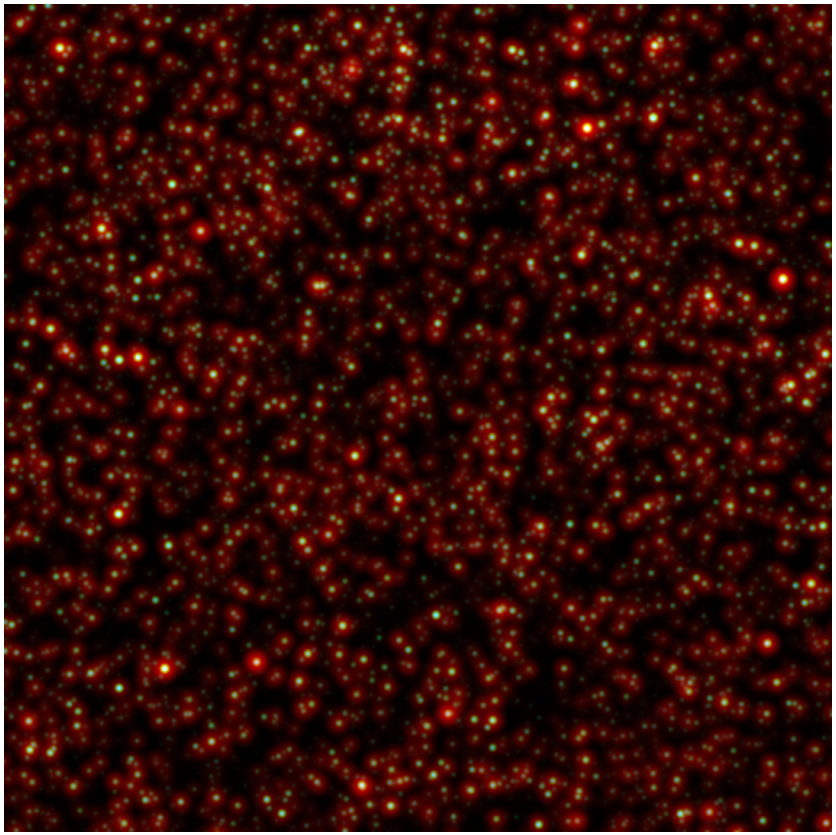

R - 2000μm, G – 850μm, B – 650μm

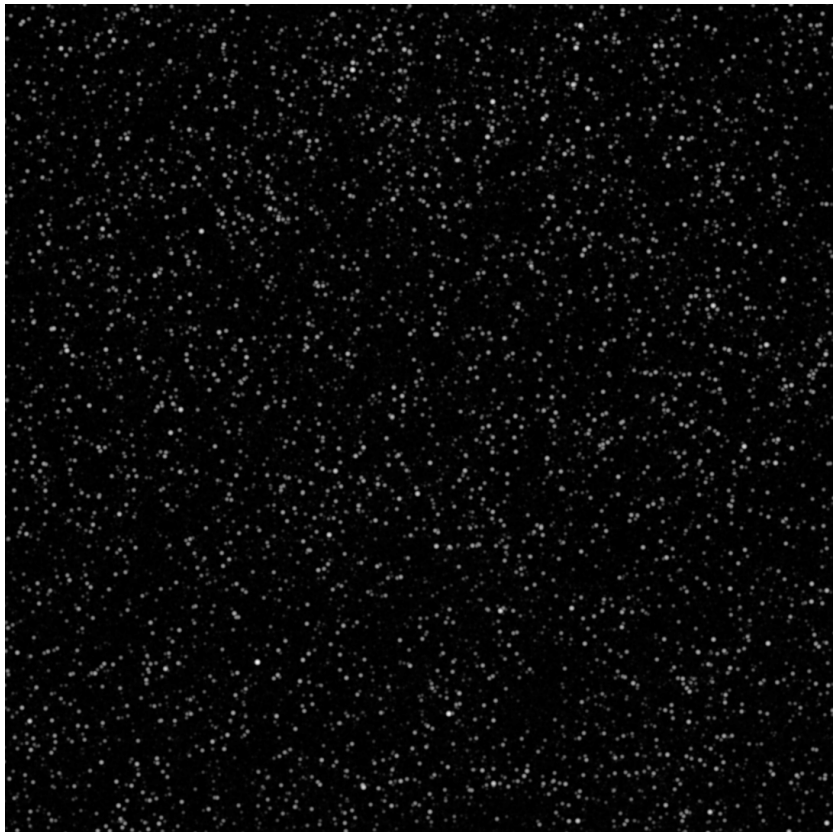

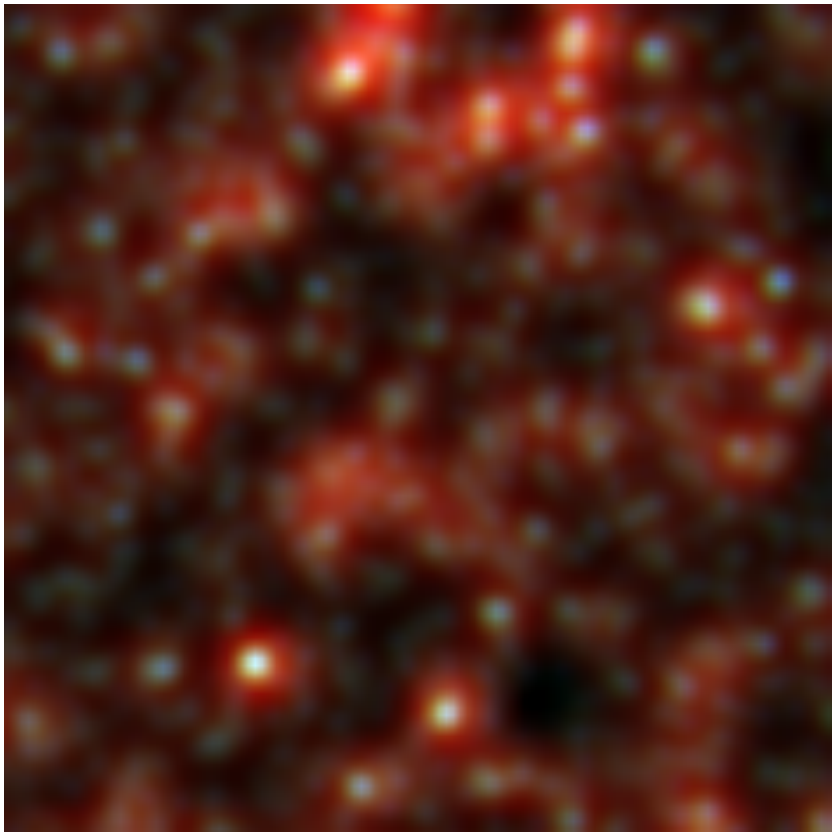

250μm, A1758

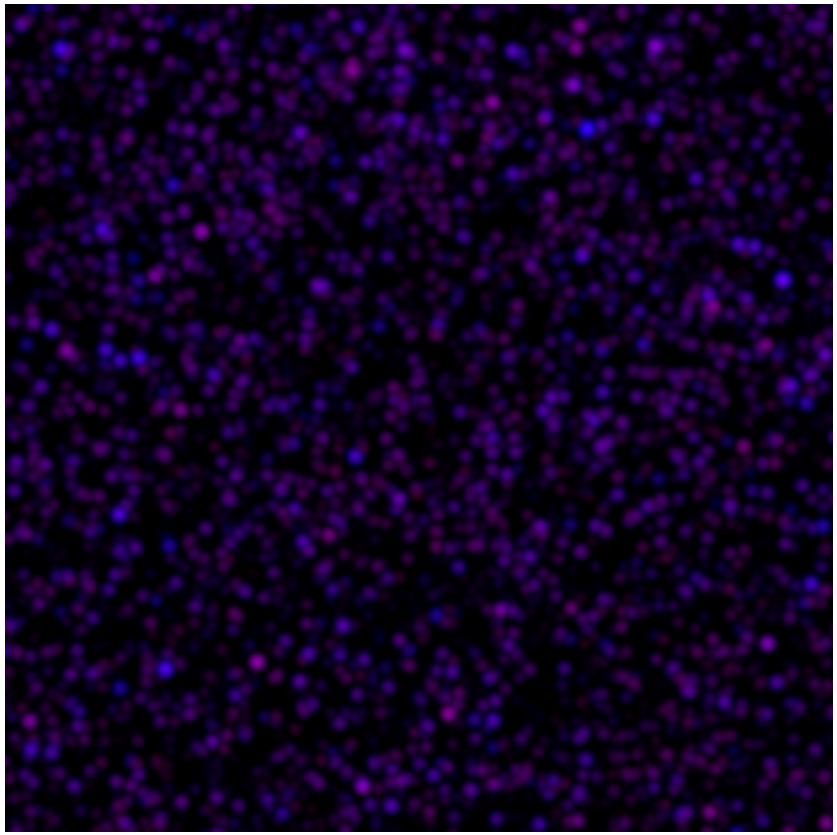

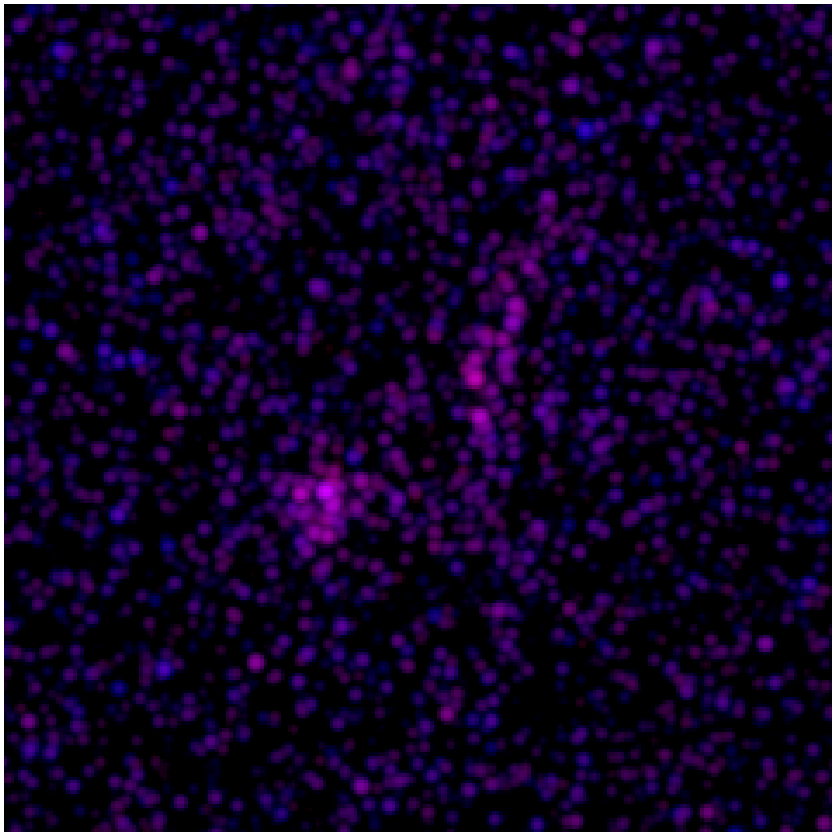

The end